Article

TRANSPARENT PROCESS OPEN ACCESS

THE EMBO JOURNAL

Wnt activity and basal niche position sensitize intestinal stem and progenitor cells to DNA damage

Si Tao[1,2,3], Duozhuang Tang[1], Yohei Morita[1], Tobias Sperka[1], Omid Omrani[1], André Lechel[4,†], Vadim Sakk[4], Johann Kraus[5], Hans A Kestler[1,5], Michael Kühl[2,*] & Karl Lenhard Rudolph[1,6,**]

Abstract

Aging and carcinogenesis coincide with the accumulation of DNA damage and mutations in stem and progenitor cells. Molecular mechanisms that influence responses of stem and progenitor cells to DNA damage remain to be delineated. Here, we show that niche positioning and Wnt signaling activity modulate the sensitivity of intestinal stem and progenitor cells (ISPCs) to DNA damage. ISPCs at the crypt bottom with high Wnt/β-catenin activity are more sensitive to DNA damage compared to ISPCs in position 4 with low Wnt activity. These differences are not induced by differences in cell cycle activity but relate to DNA damage-dependent activation of Wnt signaling, which in turn amplifies DNA damage checkpoint activation. The study shows that instructed enhancement of Wnt signaling increases radio-sensitivity of ISPCs, while inhibition of Wnt signaling decreases it. These results provide a proof of concept that cell intrinsic levels of Wnt signaling modulate the sensitivity of ISPCs to DNA damage and heterogeneity in Wnt activation in the stem cell niche contributes to the selection of ISPCs in the context of DNA damage.

Keywords DNA damage; intestinal progenitor cells; intestinal stem cells; telomeres; Wnt

Subject Categories Development & Differentiation; Signal Transduction; Stem Cells

DOI 10.15252/embj.201490700 | Received 29 November 2014 | Revised 22 December 2014 | Accepted 23 December 2014 | Published online 21 January 2015

The EMBO Journal (2015) 34: 624–640

Introduction

There is increasing evidence that the functionality of stem cells in adult tissues decreases during aging (for review see Liu & Rando, 2011; Sperka *et al*, 2012), which seems to be driven by both age-dependent alterations in stem cell self-renewal pathways and the accumulation of molecular damages. An accumulation of DNA damage occurs in various tissues and in stem cells of aging mice and humans (Herbig *et al*, 2006; Rossi *et al*, 2007; Jiang *et al*, 2008; Rube *et al*, 2011). DNA damage impairs stem cell maintenance and function in adult tissues (Rudolph *et al*, 1999; Armanios *et al*, 2007; Rossi *et al*, 2007; Hoeijmakers, 2009; Sperka *et al*, 2012; Tumpel & Rudolph, 2012). The accumulation of DNA damage and mutations in stem and progenitor cells also contribute to cancer formation during aging, and it was shown that adult tissue stem cells represent the cell type of origin of cancer formation in mouse models (Barker *et al*, 2009). Emerging data indicate that adult tissue stem cells accumulate mutations that contribute to cancer initiation during aging (Busque *et al*, 2012; Jan *et al*, 2012; Welch *et al*, 2012; Genovese *et al*, 2014; Jaiswal *et al*, 2014; Xie *et al*, 2014).

Molecular mechanisms that influence checkpoint induction and selection of mutant stem and progenitor cells in the context of DNA damage and aging remain yet to be delineated. It is currently not known whether stem cell self-renewal pathways influence the induction of DNA damage checkpoints in adult tissue stem and progenitor cells. Canonical Wnt/β-catenin signaling represents a critical self-renewal pathway, which is required for the maintenance of stem cells in adult mammalian tissues (Reya & Clevers, 2005; van Amerongen *et al*, 2012). Inactivation of essential components of canonical Wnt signaling results in defects in the maintenance of intestinal stem cells (Fevr *et al*, 2007; de Lau *et al*, 2011) and hematopoietic stem cells (HSCs) (Reya *et al*, 2003; Fleming *et al*, 2008; Luis *et al*, 2009). However, also the over-activation of canonical Wnt signaling is detrimental for stem cell maintenance and leads to premature exhaustion of HSCs (Scheller *et al*, 2006; Huang *et al*, 2009; Lane *et al*, 2010).

1 Leibniz Institute for Age Research – Fritz Lipmann Institute e.V. (FLI), Jena, Germany
2 Institute of Biochemistry and Molecular Biology, Ulm University, Ulm, Germany
3 International Graduate School in Molecular Medicine Ulm, Ulm University, Ulm, Germany
4 Cooperation Group between the Leibniz Institute for Age Research, Ulm University, Ulm, Germany
5 Medical Systems Biology Unit, Ulm University, Ulm, Germany
6 Research Group on Stem Cell Aging, Jena University Hospital (UKJ), Jena, Germany
*Corresponding author. Tel: +49 731 500 23283; Fax: +49 731 500 23277; E-mail: michael.kuehl@uni-ulm.de
**Corresponding author. Tel: +49 3641 6563 50/52; Fax: +49 3641 6563 50/52; E-mail: klrudolph@fli-leibniz.de
†Present address: Department of Gastroenterology, University Hospital Ulm, Ulm, Germany

Alterations in Wnt signaling were implicated in aging of adult tissues (Brack *et al*, 2007; Liu *et al*, 2007; Ye *et al*, 2007). Specifically, it was shown that increased activity of canonical Wnt/β-catenin signaling leads to the dysfunction of muscle stem cells during aging (Brack *et al*, 2007). In the small intestine, Paneth cells build the stem cell niche and provide key signals such as Wnt ligands for the maintenance of intestinal stem cells. Since Paneth cells exclusively sit at the bottom of the crypts, they create a Wnt gradient in the crypts with highest level at the crypt base and lower levels toward the upper part of the crypts (van der Flier *et al*, 2009; Itzkovitz *et al*, 2012). Despite numerous findings on the role of Wnt signaling in controlling the maintenance and plasticity of intestinal stem and progenitor cells (ISPCs), mechanistic studies on the influence of Wnt/β-catenin signaling on the maintenance of ISPC in the context of DNA damage have not been reported. Here, we provide experimental evidence that niche positioning-dependent differences in the level of canonical Wnt/β-catenin signaling modulate the sensitivity of ISPCs to DNA damage in the intestinal epithelium of mice. Cells with high Wnt/β-catenin activity (Wnt^{hi}) at the crypt base are more sensitive to DNA damage-induced depletion compared to Wnt^{lo} border cells at position 4. The increased sensitivity of Wnt^{hi} cells to DNA damage is not associated with differences in cell cycle activity but involves a feed-forward loop of transient Wnt activation in response to DNA damage and amplification of DNA damage checkpoints in cells with high Wnt signaling activity. Of note, instructed activation of canonical Wnt signaling enhances radio-sensitivity of ISPCs, while inhibition of Wnt signaling decreases it, both in cell culture and *in vivo*. These findings could be relevant for the accumulation of genetic alterations and the clonal selection of stem and/or progenitor cells in the context of DNA damage during aging and carcinogenesis as well as for therapeutic targeting of cancer stem cells with elevated levels of DNA damage.

Results

Positioning within the niche and levels of LGR5 expression discriminate intestinal ISPCs with different Wnt/β-catenin signaling activity

Recent studies revealed a high plasticity of ISPCs in the basal crypts of the intestinal epithelium. It was shown in lineage tracing experiments that LGR5-positive cells at the crypt base in position 1 and 2 represent intestinal stem cells (Barker *et al*, 2007). In addition, $LGR5^+$ cells in the border region (position 3/4 of the crypt) have true stem cell activity and can replace stem cells at the crypt base (Ritsma *et al*, 2014). However, it was also shown that LGR5-negative TA cells can revert to organoid-forming stem cells in culture when exposed to Wnt3A (Sato *et al*, 2011) as well as in response to tissue injury *in vivo* (van Es *et al*, 2012), but these events are rare and $LGR5^+$ cells were found to be essential for intestinal regeneration and mouse survival in response to irradiation (IR) (Metcalfe *et al*, 2014). The main aim of this study was to delineate the potential influence of Wnt/β-catenin signaling on the survival of the total population of ISPCs in response to DNA damage rather than to re-investigate the discrimination of intestinal stem and progenitor cells and the plasticity of early progenitors to convert into stem cells or vice versa. Therefore, $LGR5^+$ cells in position 1–4 cells are altogether referred to as "stem and progenitor cells (ISPCs)" from here on.

$LGR5^+$ ISPCs are placed in between and adjacent to the Paneth cells in position 1–4 of the crypt base (Barker *et al*, 2007). Paneth cells produce the Wnt/β-catenin stimulatory ligand Wnt3, which represents an essential factor for adapting freshly isolated $LGR5^+$ ISPCs to cell culture (Sato *et al*, 2011). Although Paneth cells are dispensable for the maintenance of intestinal stem cells *in vivo* (Kim *et al*, 2012), it was shown that intestinal stem cells that are located in between the Paneth cells at the very bottom of the crypts (also known as "crypt base columnar stem cells—CBCs" located at position 1 and 2 of the crypt base) express higher levels of Wnt target genes such as *Lgr5*, *Ascl2*, and *Sox9* compared to position 4 cells that are located above the Paneth cells and are therefore also known as "border cells" (van der Flier *et al*, 2009; Itzkovitz *et al*, 2012; Ritsma *et al*, 2014). These previous studies indicated that Paneth cells generate a Wnt gradient-exposing cells at the crypt base that are surrounded by multiple Paneth cells to a higher Wnt3 level than border cells that are located above the Paneth cells, thus only contacting 1 or 2 Paneth cells. In agreement with previous studies, immunofluorescence staining of LGR5-GFP expression and Musashi-1 (Msi1) (both direct targets of Wnt/β-catenin signaling) confirmed higher Wnt signal activity in position 1–2 cells compared to cells at position 4 (Fig 1A–D). Fluorescence-activated cell sorting (FACS) of freshly isolated crypts showed that intestinal crypts contained $LGR5^+$ cells with relatively higher ($LGR5^{hi}$) or lower ($LGR5^{lo}$) LGR5-GFP expression (Fig 1E). Aside from the stability of the GFP protein, it was shown that transcriptional control of LGR5 expression, directly targeted by Wnt/β-catenin signaling, contributes to differences in the level of GFP expression in the population of LGR5-positive intestinal ISPCs in this reporter strain (Munoz *et al*, 2012). To determine whether FACS can be used to separate ISPCs with different intrinsic levels of Wnt signaling activity, four subpopulations of cells were FACS-purified from the intestinal epithelium of the LGR5-GFP reporter mouse strain based on the level of GFP expression: (i) $LGR5^{hi\text{-}high}$, (ii) $LGR5^{hi\text{-}low}$, (iii) $LGR5^{lo\text{-}high}$, (iv) $LGR5^{lo\text{-}low}$ (Fig 1F). qPCR analysis revealed that the LGR5-GFP expression level correlated with the expression level of several Wnt target genes including *Axin2*, *Ascl2*, and *Msi1* (Fig 1G–I), indicating that FACS can be employed to efficiently purify ISPCs with different levels of Wnt signaling. Wnt activity showed an inverse correlation with expression of some differentiation markers (*Fabp1*, *Chga*, *Dclk1*, Supplementary Fig S1). Together, these experiments revealed that FACS purification based on the LGR5 reporter expression separates ISPCs with high or low Wnt signaling activity and immunostaining indicated a correlation between the level of Wnt target gene expression (*LGR5* and *Msi*) and the localization of cells in the basal crypt (position 1/2 > position 4).

Telomere dysfunction associates with suppression of Wnt signaling in ISPCs of aging telomerase-deficient mice

Homozygous deletion of the RNA component of telomerase (*mTerc*) accelerates telomere shortening and leads to an age-dependent accumulation of telomere dysfunction in the third generation of knockout mice (G3 $mTerc^{-/-}$) compared to wild-type mice ($mTerc^{+/+}$). As DNA damage accumulates in G3 $mTerc^{-/-}$ mice, we here used these mice as a model of age-dependent DNA damage accumulation.

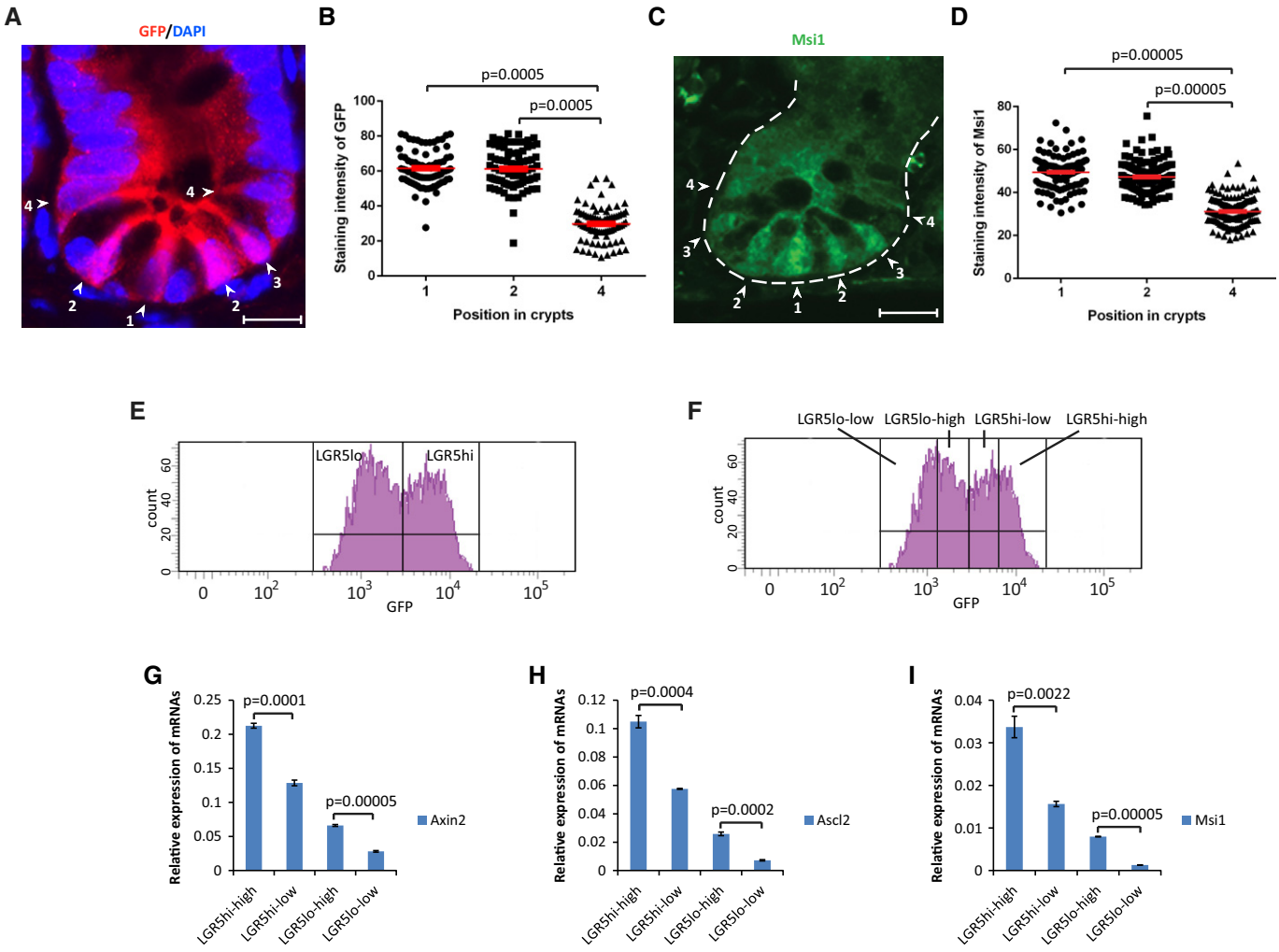

Figure 1. Niche-dependent Wnt activity in intestinal stem and progenitor cells.

A Representative immunofluorescence staining of GFP of small intestinal tissue of LGR5-GFP knock-in (LGR5-GFP^{ki}) mice. Arrowheads and numbers indicate ISPC positions in the crypts. Scale bar: 20 μm.

B Quantification of GFP staining intensity of intestinal stem and progenitor cells (ISPCs) at indicated positions in basal crypts of LGR5-GFP^{ki} mice (n = 80 crypts from four mice). Each dot presents one cell. Red lines: mean values ± SEM. Unpaired two-tailed Student's t-test.

C Representative immunofluorescence staining of Msi1 of small intestinal tissue of young $mTerc^{+/+}$ mice. Dashed line outlines a crypt. Arrowheads and numbers indicate ISPC positions in the crypts. Scale bar: 20 μm.

D Quantification of Msi1 staining intensity of ISPCs at indicated positions in basal crypts of young $mTerc^{+/+}$ mice (n = 150 crypts from three mice). Each dot presents one cell. Red lines: mean values ± SEM. Unpaired two-tailed Student's t-test.

E Representative FACS plots showing gating of LGR5^{hi} and LGR5^{lo} populations within the LGR5^{+} (GFP-positive) cell gating.

F Representative FACS plots showing gating of LGR5$^{hi\text{-}high}$, LGR5$^{hi\text{-}low}$, LGR5$^{lo\text{-}high}$, and LGR5$^{lo\text{-}low}$ populations within the LGR5^{hi} gating.

G–I mRNA expression of indicated genes relative to *GAPDH* in LGR5$^{hi\text{-}high}$, LGR5$^{hi\text{-}low}$, LGR5$^{lo\text{-}high}$, and LGR5$^{lo\text{-}low}$ populations (n = 3 mice). Mean values ± SEM are given. Unpaired two-tailed Student's t-test.

Telomere dysfunction in aging G3 $mTerc^{-/-}$ mice induces p53-dependent impairments of stem cell maintenance and premature aging of somatic tissues (Choudhury *et al*, 2007; Begus-Nahrmann *et al*, 2009; Sperka *et al*, 2011). The intestinal epithelium is an organ compartment with very high rates of cell turnover, which is strongly affected by aging-associated accumulation of telomere dysfunction in telomerase-deficient mice (Choudhury *et al*, 2007; Schaetzlein *et al*, 2007; Sperka *et al*, 2011).

The canonical Wnt signaling pathway has been identified as a major regulator of stem cell maintenance in the intestinal epithelium (Reya & Clevers, 2005). To see whether this pathway is affected in response to telomere dysfunction, gene expression analysis was employed. mRNA expression analysis of components of the canonical Wnt/β-catenin signaling pathway revealed a significant suppression of various components of the Wnt signaling pathway in freshly isolated basal intestinal crypts of 12- to 16-month-old G3 $mTerc^{-/-}$ mice compared to age-matched $mTerc^{+/+}$ mice (Fig 2A). A significant suppression of *Axin2* was also detected in freshly isolated, highly purified, LGR5^{+} ISPCs from 12- to 16-month-old G3 $mTerc^{-/-}$ mice compared to age-matched $mTerc^{+/+}$ mice (Fig 2B).

Telomere dysfunction was previously shown to repress the ability of LGR5^{+} ISPCs to grow organoids in cell culture (Sperka

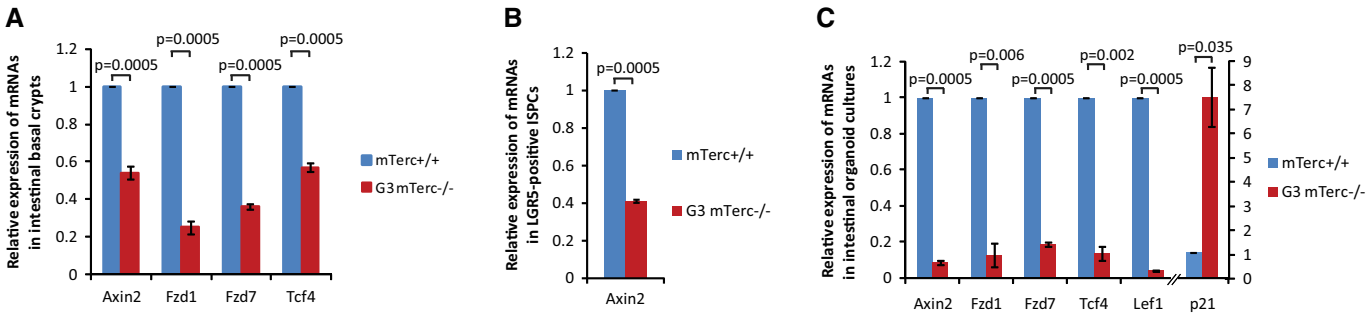

Figure 2. Suppression of Wnt signaling in intestinal basal crypts and ISPCs of aging telomerase-deficient mice.

A mRNA expression of indicated components of the canonical Wnt/β-catenin pathway in freshly isolated small intestinal crypts of 12- to 16-month-old G3 *mTerc*$^{-/-}$ mice and age-matched *mTerc*$^{+/+}$ mice (n = 5 mice per group).

B *Axin2* mRNA expression in LGR5^{+} cells of 12- to 16-month-old G3 *mTerc*$^{-/-}$ mice and *mTerc*$^{+/+}$ mice (n = 3 mice per group).

C mRNA expression of indicated components of the canonical Wnt/β-catenin pathway and of the p53 target gene *p21* in cultured crypts of 2-month-old G3 *mTerc*$^{-/-}$ mice and *mTerc*$^{+/+}$ mice (n = 3 mice per group).

Data information: Mean values ± SEM are given. Unpaired two-tailed Student's *t*-test.

et al, 2011). To test whether suppression of Wnt signaling was associated with this deficiency, intestinal organoids were re-derived from primary cultures after two passages, 18 days after initiating cultures from freshly isolated basal crypts from 2-month-old G3 *mTerc*$^{-/-}$ mice or *mTerc*$^{+/+}$ mice. mRNA analysis revealed a significant suppression in the expression of several components of the Wnt pathway, but an increase in the expression of the DNA damage marker *p21* in organoids derived from intestinal crypts of G3 *mTerc*$^{-/-}$ mice compared to *mTerc*$^{+/+}$ mice (Fig 2C).

Telomere dysfunction leads to preferential depletion of ISPCs with high Wnt activity

Together, the above data showed that telomere dysfunction and activation of DNA damage signals associate with the suppression of canonical Wnt/β-catenin signaling in the ISPC compartment. DNA damage accumulates in the intestine of aging G3 *mTerc*$^{-/-}$ mice, and this leads to impairments in the maintenance of ISPCs and an increasing atrophy of the intestinal epithelium in aging G3 *mTerc*$^{-/-}$ mice (Begus-Nahrmann *et al*, 2009; Sperka *et al*, 2011). In agreement with these studies, FACS analysis revealed a significant depletion of ISPCs in 12- to 16-month-old G3 *mTerc*$^{-/-}$ mice compared to age-matched *mTerc*$^{+/+}$ mice, but not in 2- to 3-month-old mice (Fig 3A, C and D, Supplementary Fig S2). Interestingly, this age-dependent decrease in ISPCs was more pronounced in the fraction of LGR5^{hi} cells (Fig 3B and E–G). Moreover, within the LGR5^{hi} cells, the subpopulation of LGR5$^{hi\text{-}high}$ cells was preferentially depleted compared to the subpopulation of LGR5$^{hi\text{-}low}$ cells (Fig 3H–J, see Fig 1F for gating of subpopulations from the total population of LGR5^{+} cells). Histological analysis indicated that surviving LGR5^{+} cells in 9-month-old G3 *mTerc*$^{-/-}$ mice exhibited weaker GFP staining intensity and were mostly located at position 4 above the Paneth cells, whereas LGR5^{+} cells at the crypt base that were located in between the Paneth cells (position 1 and 2) were preferentially depleted (Fig 3K–O).

The use of multiple markers confirmed that telomere dysfunction led to a depletion of ISPCs at position 1–2 of the basal crypt including: (i) morphological markers depicting ISPCs as small spindle-like cells located adjacent to Paneth cells at the crypt base (Barker *et al*, 2012) (Fig 4A–C, Supplementary Fig S3), (ii) PCNA immunofluorescence distinguishing proliferative ISPCs from post-mitotic Paneth cells (Fig 4D–F), (iii) Msi1 immunofluorescence staining for ISPCs at position 1–4 of the basal crypt (Kayahara *et al*, 2003; Rezza *et al*, 2010) (Fig 4G–I), and (iv) olfactomedin 4 (*Olfm4*) *in situ* hybridization: *Olfm4* is a Notch target gene but is not directly regulated by Wnt (van der Flier *et al*, 2009) and labels ISPCs in position 1–4 of basal crypts (Fig 4J and K).

Figure 3. Telomere dysfunction leads to preferential depletion of ISPCs with high Wnt activity at the crypt base.

A–J Flow cytometry analysis of freshly isolated crypt cells from the small intestine of young (2–3 month) and old (12–16 month) LGR5-GFP^{ki}, *mTerc*$^{+/+}$ mice and LGR5-GFP^{ki}, G3 *mTerc*$^{-/-}$ mice (n = 4 mice per group). (A, B, D, E, H, I) Representative FACS plots depicting the analysis of LGR5^{+} cells. Note the reduction in LGR5^{+} cells in G3 *mTerc*$^{-/-}$ mice with the remaining cells showing almost exclusively weak expression of GFP (LGR5^{lo}) and that within the fraction of LGR5^{hi} cells, the cells with high LGR5-reporter activity (LGR5$^{hi\text{-}high}$) are preferentially depleted in response to IR. (C, F) Quantification of (C) the number of LGR5^{+} cells and (F) the number of LGR5^{hi} and LGR5^{lo} cells. (G) Quantification of the percentage of LGR5^{hi} cells and LGR5^{lo} cells within the fraction of LGR5^{+} cells. (J) Quantification of the survival rate of LGR5$^{hi\text{-}high}$ cells and LGR5$^{hi\text{-}low}$ cells within the fraction of LGR5^{hi} cells comparing old G3 *mTerc*$^{-/-}$ mice to *mTerc*$^{+/+}$ mice.

K–O Immunofluorescence staining of GFP in basal crypts of 9-month-old LGR5-GFP^{ki}, G3 *mTerc*$^{-/-}$ mice and age-matched LGR5-GFP^{ki}, *mTerc*$^{+/+}$ mice (n = 2 mice per group). (K, L) Representative pictures are given. Dashed lines outline the crypts. Arrowheads and numbers indicate ISPC positions in the crypts. Scale bar: 20 μm. (M) Quantification of absolute number of GFP^{+} ISPCs at indicated positions at the crypt base per 50 crypts. (N) The histogram depicts the depletion rate (%) of LGR5^{+} cells in LGR5-GFP^{ki}, G3 *mTerc*$^{-/-}$ mice compared to age-matched LGR5-GFP^{ki}, *mTerc*$^{+/+}$ mice at indicated positions in the basal crypts. (O) Quantification of GFP staining intensity of ISPCs at indicated positions in positively stained basal crypts. Note that the staining intensity of position 4 cells is equal in *mTerc*$^{+/+}$ mice and G3 *mTerc*$^{-/-}$ mice and is significantly lower than position 1 and 2 cells of *mTerc*$^{+/+}$ mice.

Data information: Mean values ± SEM are given. Unpaired two-tailed Student's *t*-test.

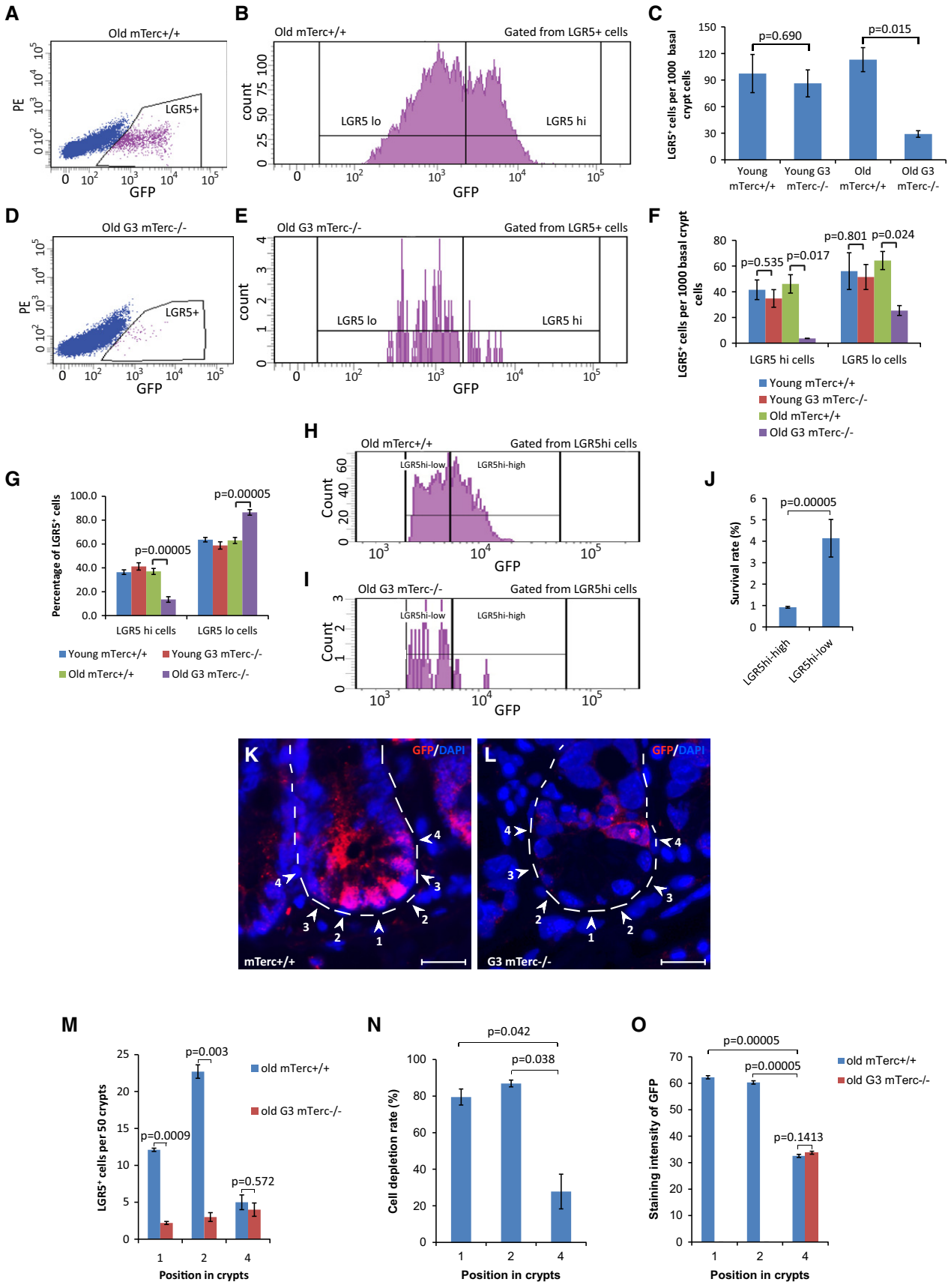

Figure 3.

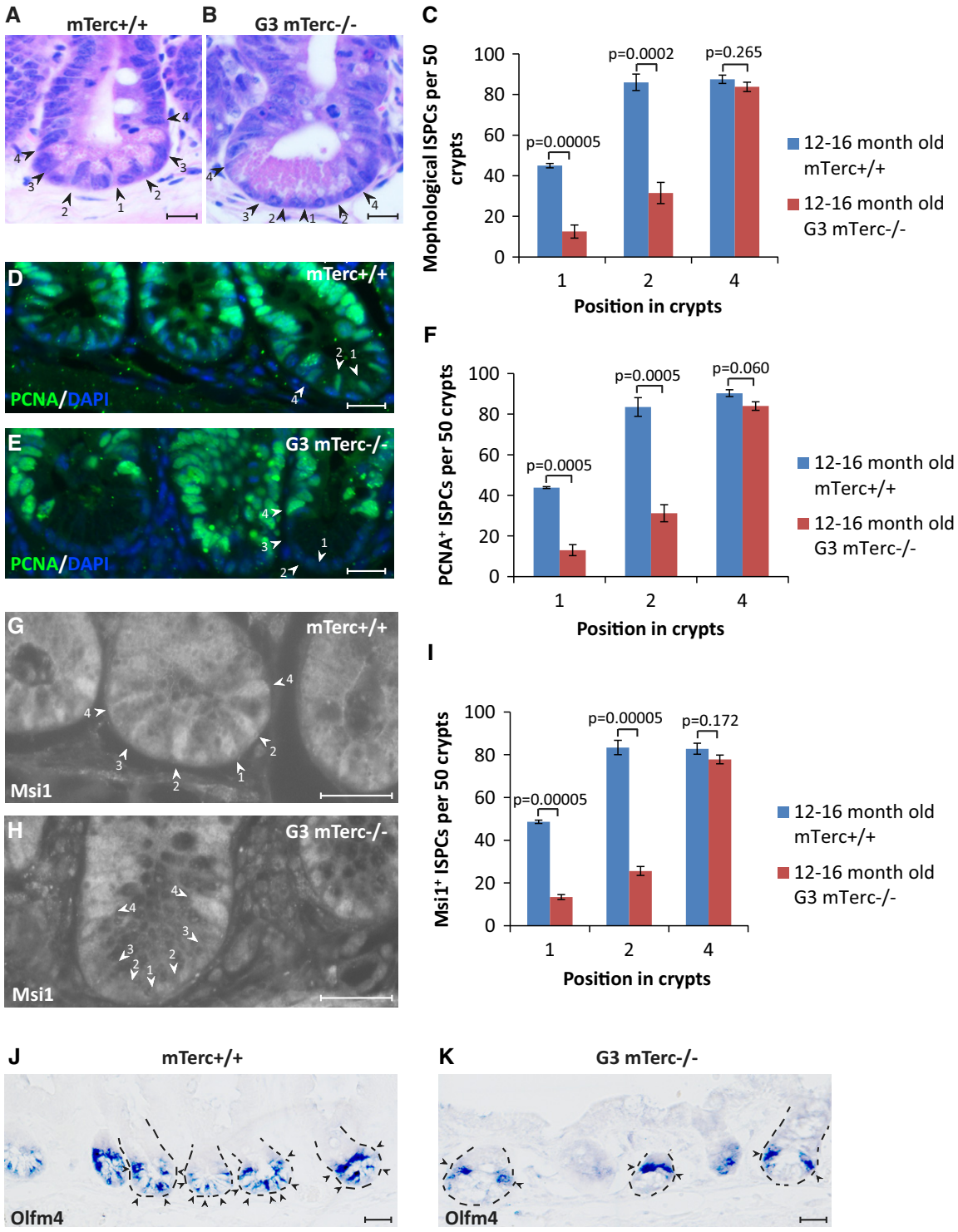

Figure 4. Telomere dysfunction leads to preferential depletion of position 1 and 2 cells at the crypt bottom in between Paneth cells.

A–I Staining of small intestinal tissue sections of 12- to 16-month-old G3 *mTerc*$^{-/-}$ mice and age-matched *mTerc*$^{+/+}$ mice (n = 4–5 mice per group). Representative pictures of (A, B) H&E staining, (D, E) PCNA staining, and (G, H) Msi1 staining are given. Arrowheads and numbers indicate the position of ISPCs in the basal crypts. Scale bars: 20 μm. (C, F, I) Quantification of the absolute numbers of ISPCs at the indicated positions in the crypt base per 50 crypts as determined by counting of (C) spindle-shaped cells in between and adjacent to the Paneth cells, cells staining positive for (F) PCNA or (I) Msi1. Mean values ± SEM are given. Unpaired two-tailed Student's t-test.

J, K Representative pictures of Olfm4 *in situ* hybridization on small intestinal sections of 9-month-old G3 *mTerc*$^{-/-}$ mice (K) and age-matched *mTerc*$^{+/+}$ (J) mice. Arrowheads point to positive cells. Dashed lines outline the crypts. Note that the remaining ISPCs in G3 *mTerc*$^{-/-}$ mice were mostly located in position 4 above the Paneth cells. Scale bar: 20 μm.

γ-irradiation-induced DNA damage leads to preferential depletion of ISPCs with high Wnt signaling

To determine the DNA damage sensitivity of ISPCs in a different model, we analyzed the number of ISPCs in the intestine of 3-month-old *mTerc*$^{+/+}$ mice in response to acute exposure to γ-irradiation. Immunohistochemistry analysis showed a rapid depletion of PCNA-positive (PCNA^{+}) ISPCs at the crypt base (position 1 and 2 at 24–48 h after IR) but a recovery of these cells at day 4–6 after IR (Fig 5A–G). In contrast, PCNA^{+} cells located above the

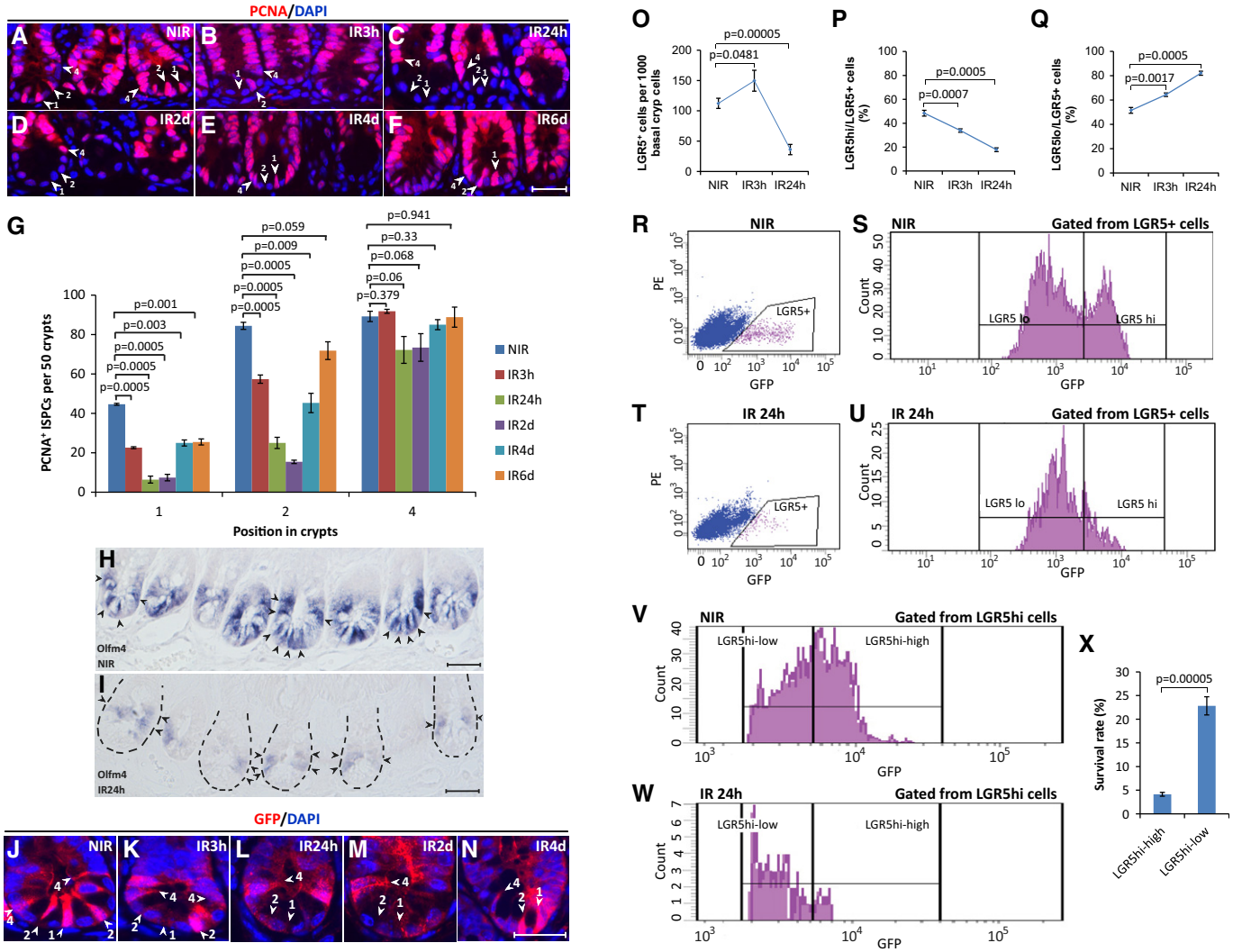

Figure 5. γ-irradiation leads to preferential depletion of ISPCs with high Wnt signaling activity.

A–I Three-month-old *mTerc*$^{+/+}$ mice were exposed to 12 Gy γ-irradiation. Small intestinal tissue was collected at indicated time points after IR (n = 5 mice per group). (A–F) Representative pictures of PCNA staining. Arrowheads and numbers indicate ISPC positions in the crypts. Scale bar: 20 μm. Note the depletion of PCNA^{+} CBC cells in position 1 and 2 in between the Paneth cells at 3–48 h after IR and the regeneration of these cells at 4–6 days after IR. (G) Quantification of PCNA^{+} ISPCs at the indicated positions in basal crypts at the indicated time points after IR. Mean values ± SEM are given. (H, I) Representative pictures of Olfm4 *in situ* hybridization. Arrowheads point to positive cells. Dashed lines outline the crypts in irradiated samples. Scale bar: 20 μm. Note the selective survival of ISPCs above the Paneth cells at 24 h after IR.

J–X Three-month-old LGR5-GFP^{ki}, *mTerc*$^{+/+}$ mice were exposed to 12 Gy γ-irradiation. Small intestinal tissue was collected at indicated time points after IR. (J–N) Representative pictures of GFP staining at indicated time points after irradiation. Arrowheads and numbers indicate ISPC positions in the crypts. Scale bar: 20 μm. (O–X) Flow cytometry analysis of freshly isolated basal crypt cells at the indicated time points after IR (n = 4–10 mice per group). (O) The histogram depicts the number of LGR5^{+} cells in freshly isolated basal crypts at the indicated time point after IR. (P, Q) Flow cytometry analysis was used to determine the percentage of (P) LGR5^{hi} cells and (Q) LGR5^{lo} cells within the fraction of LGR5^{+} cells. (R-W) Representative FACS plots of small intestinal crypt cells of non-irradiated mice, 24 h after irradiation. Note the reduction in LGR5^{+} cell in irradiated mice with the remaining cells showing almost exclusively weak expression of GFP (LGR5^{lo}). (X) Quantification of the survival rate of LGR5$^{hi\text{-}high}$ cells and LGR5$^{hi\text{-}low}$ cells within the fraction of LGR5^{hi} cells comparing irradiated mice to non-irradiated mice. Note the preferential depletion of LGR5$^{hi\text{-}high}$ cells within LGR5^{hi} cell population upon IR. Mean values ± SEM are given. NIR, non-irradiated; IR, irradiated.

Data information: In (G, O–Q, X), unpaired two-tailed Student's t-test was applied.

Paneth cells (position 4) were maintained after IR (Fig 5A–G). To verify that γ-irradiation led to the depletion of position 1–2 cells, Wnt-independent markers (*Olfm4*, Fig 5H and I) and Wnt-dependent markers (LGR5 and Msi1, Fig 5J–N, Supplementary Fig S4A–C) were employed. Staining for GFP expression in LGR5-GFP^{ki} mice indicated a depletion of cells at the bottom of the crypt at position 1 and 2 reaching a maximum at 24 h to 2 days after IR (Fig 5J–N), and a preferential maintenance of position 4 cells with weaker GFP staining intensity (Supplementary Fig S4D). At later time points (4 days after IR), a recovery of LGR5$^+$ cells at position 1–2 occurred (Fig 5N). Staining of intestinal crypts for the expression of *Olfm4* and Msi1 confirmed the depletion of ISPCs at the crypt bottom at 24 h after IR (Fig 5H and I, Supplementary Fig S4A–C).

To quantify the survival of LGR5^{lo} cells and LGR5^{hi} cells, FACS was used to analyze intestinal crypt cells from irradiated mice at different time points after IR (3–24 h). At 3 h after IR, there was a transient increase of LGR5$^+$ cells indicative of an IR-mediated induction of Wnt signaling (Fig 5O). However, 24 h after IR, a significant reduction of LGR5$^+$ cells occurred (Fig 5O) predominantly affecting the subpopulation of LGR5^{hi} cells compared to LGR5^{lo} cells (Fig 5P–U). Gating of sub-populations within the population of LGR5^{hi} cells revealed that the LGR5$^{hi\text{-}high}$ cells were preferentially depleted compared to the LGR5$^{hi\text{-}low}$ cells (Fig 5V–X, see Fig 1F for gating of subpopulations from the total population of LGR5$^+$ cells).

To test whether differences in cell cycle [a known factor influencing the sensitivity of cells to DNA damage (Ren *et al*, 2002)] would correlate with increased DNA damage sensitivity of LGR5^{hi} cells compared to LGR5^{lo} cells, different cell cycle markers were employed. Staining for Ki-67 and PCNA did not reveal significant differences in cell cycle activity of position 1 and 2 cells compared to position 4 cells (Supplementary Fig S5A–D). Similarly, FACS analysis of freshly isolated LGR5$^+$ ISPCs from non-irradiated and irradiated (24 h after IR) LGR5-GFP^{ki} mice did not reveal significant differences in the cell cycle profile of LGR5^{hi} cells compared to LGR5^{lo} cells (Supplementary Fig S5E–I). Together, these data indicated that cell cycle differences did not account for the increased DNA damage sensitivity of LGR5^{hi} cells compared to LGR5^{lo} cells.

Enhancement of p53-dependent apoptosis in response to irradiation in LGR5^{hi} cells compared to LGR5^{lo} cells

LGR5^{hi} cells and LGR5^{lo} cells from 3-month-old mice were FACS-purified 6 h after IR. Gene expression array analysis of non-irradiated and 12 Gy γ-irradiated mice (6 h after IR, n = 4–5 samples per group) showed a significant increase in the number of genes that were induced or suppressed in response to γ-irradiation in LGR5^{hi} cells compared to LGR5^{lo} cells (2,294 versus 567, $P = 1.3 \times 10^{-25}$, Fig 6A). A total of 266 genes were regulated in both cell populations in response to IR. However, the level of IR-induced changes in the expression of these genes was significantly higher in LGR5^{hi} cells compared to LGR5^{lo} cells (median absolute fold change 4.9 versus 3.8, $P < 0.0001$, Fig 6A). Among the genes that were more strongly induced in LGR5^{hi} cells versus LGR5^{lo} cells was a set of apoptosis-inducing genes including the p53 targets *PUMA*, *NOXA,* and *BOK*. qPCR analysis confirmed that IR led to a stronger induction of these pro-apoptotic genes in LGR5^{hi} cells compared to LGR5^{lo} cells (Fig 6B). Enhanced activation of p53-dependent apoptosis could explain the increased sensitivity of LGR5^{hi} cells to DNA damage compared to LGR5^{lo} cells. In agreement with this interpretation, Western blot analysis of freshly isolated LGR5$^+$ cells derived from mice exposed to 12 Gy γ-irradiation (6 h after IR) revealed an enhanced expression of phosphorylated p53 and cleaved caspase-3 in LGR5^{hi} cells compared to LGR5^{lo} cells (Fig 6C, Supplementary Fig S6). TUNEL staining for apoptotic cells at 3 h after IR depicted reduced rates of apoptosis in position 4 cells compared to position 1 and 2 cells (Fig 6D and E). To test the functional role of p53 in enhancing radio-sensitivity of LGR5^{hi} cells compared to LGR5^{lo} cells, the depletion of ISPCs was determined in p53$^{-/-}$ compared to p53$^{+/+}$ LGR5-reporter mice. p53 deletion diminished IR-induced depletion of the total number of LGR5$^+$ cells (Fig 6F), but the rescue of IR-induced depletion of LGR5^{hi} cells was more pronounced compared to the rescue of IR-induced depletion of LGR5^{lo} cells (Fig 6G, I, K, M and O). Gating of sub-populations within the population of LGR5^{hi} cells showed that the rescue in radio-sensitivity in response to p53 deletion was much more pronounced in LGR5$^{hi\text{-}high}$ cells compared to the LGR5$^{hi\text{-}low}$ cells (Fig 6H, J, L, N and P, see Fig 1F for gating of subpopulations from the total population of LGR5$^+$ cells). Together, these results indicated that p53-dependent apoptosis contributes to the enhanced radio-sensitivity of ISPCs with high LGR5 expression compared to ISPCs with low LGR5 expression.

Instructed modification of canonical Wnt/β-catenin signaling activity changes the radio-sensitivity of ISPCs in culture

The experiments on irradiated mice had shown a transient increase in the total number of LGR5$^+$ cells in intestinal basal crypts at early time points after IR (3 h after IR), suggesting that Wnt signaling was transiently upregulated at early time points after IR (Fig 5O). To confirm these results, Wnt signaling activity was analyzed in ISPCs of cultured crypts derived from 3-month-old LGR5-GFP^{ki} mice at 3 and 12 h after IR. Both LGR5^{hi} and LGR5^{lo} cells exhibited a significant induction of *Axin2* at 3 h after IR compared to non-irradiated controls, but the level went back down at 12 h after IR (Supplementary Fig S7A). Together with the data on enhanced p53 activation in LGR5^{hi} cells compared to LGR5^{lo} cells (Fig 6A–C), the data on transient upregulation of Wnt signaling in response to IR suggested that DNA damage induces an activating feed-forward loop involving a transient upregulation of Wnt signaling, which in turn amplifies DNA damage responses, thus sensitizing ISPCs with intrinsically high Wnt activity to undergo DNA damage-induced depletion. According to this model, an activation or inhibition of Wnt signaling should lead to respective changes in the sensitivity of ISPCs exposed to DNA damage. To test this assumption, freshly isolated crypts were cultured and transiently exposed to modifiers of canonical Wnt signaling shortly before IR. To inhibit Wnt signaling, recombinant DKK1 protein was added to the culture medium or the concentration of R-spondin in the culture medium was reduced by 50% compared to normal conditions (Supplementary Fig S7B). To activate Wnt signaling, the GSK3 inhibitor 6-BIO was added to the culture medium (Supplementary Fig S7C). Neither the activation nor the inhibition of Wnt signaling resulted in significant changes in cell cycle activity of LGR5$^+$ cells in the crypt cultures (Supplementary Fig S7D and E). Of note, inhibition of Wnt signaling resulted in a significant decrease in radio-sensitivity of both LGR5^{hi} cells and

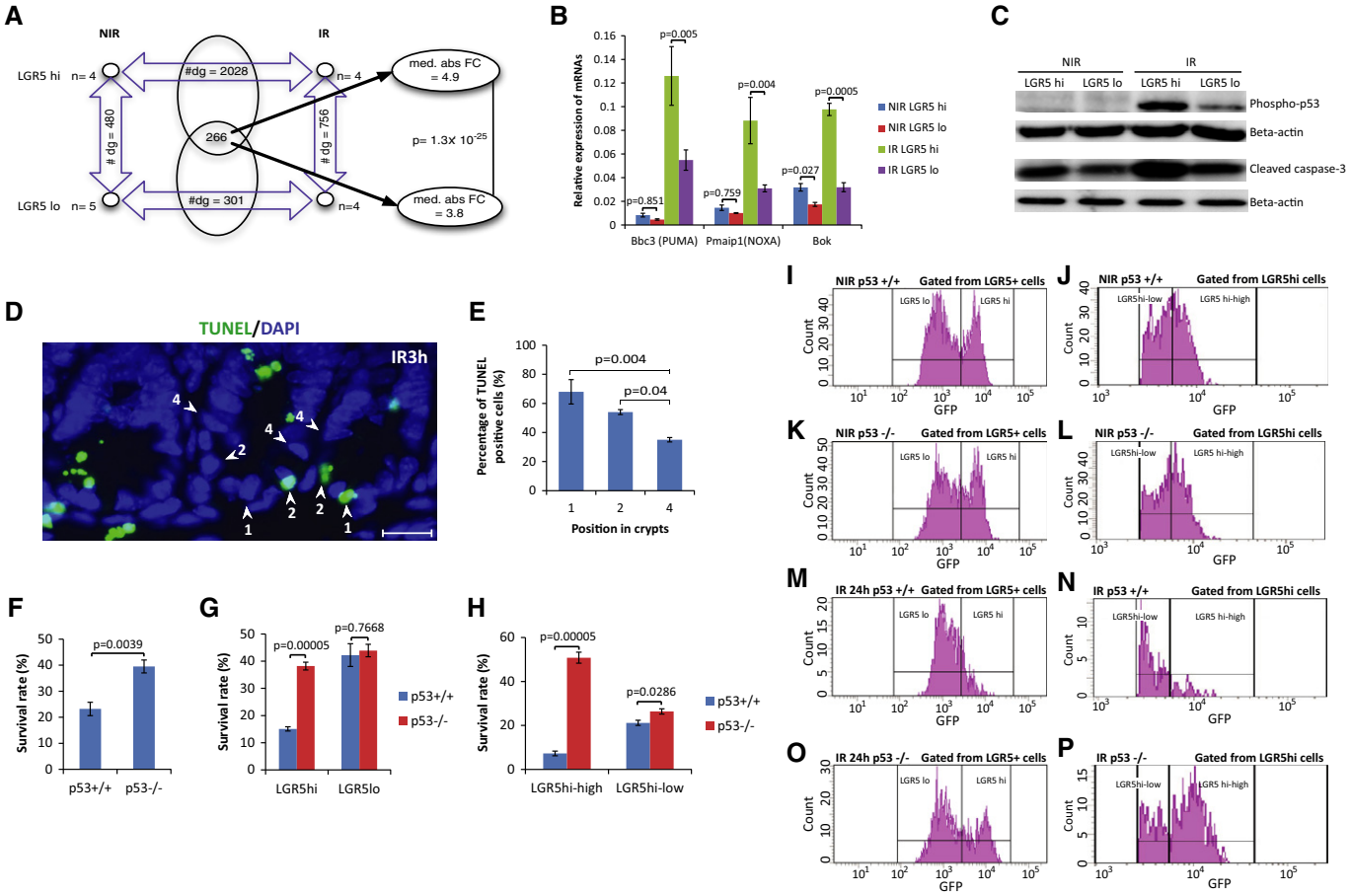

Figure 6. Enhanced induction of p53-dependent apoptosis in response to irradiation in LGR5^{hi} cells compared to LGR5^{lo} cells.

A mRNA gene expression analysis by microarray. The figure shows the number of differentially expressed genes (#dg) and the median absolute fold change (med. Abs. FC) for genes that are regulated in both LGR5^{hi} cells and LGR5^{lo} cells in response to IR (n = 4–5 samples per group). NIR, non-irradiated; IR, irradiated. Wilcoxon test.

B, C LGR5^{hi} and LGR5^{lo} cells were freshly isolated from 3-month-old LGR5-GFP^{ki} mice 6 h after 12 Gy γ-irradiation (IR) or from non-irradiated (NIR) mice (n = 3 mice per group). (B) qPCR analysis of relative mRNA expression of apoptosis-related genes compared to *GAPDH*. Mean values ± SEM are given. Unpaired two-tailed Student's t-test. (C) Representative Western blot analysis of cell lysates for the expression of phospho-p53 and cleaved caspase-3.

D, E Three-month-old *mTerc*$^{+/+}$ mice were γ-irradiated with 12 Gy. Small intestinal tissue was collected at 3 h after IR (n = 3 mice per group). (D) Representative picture of TUNEL staining. Arrowheads and numbers indicate ISPC positions in the crypts. Scale bar: 20 μm. (E) Percentage of TUNEL-positive ISPCs at indicated positions in basal crypts. Mean values ± SEM are given. Unpaired two-tailed Student's t-test.

F–P Two-month-old LGR5-GFP^{ki}, p53$^{+/+}$ mice and LGR5-GFP^{ki}, p53$^{-/-}$ mice were exposed to 12 Gy γ-irradiation (n = 4 mice per group). Basal crypts were isolated at 24 h after IR. (F–H) Flow cytometry analysis of the survival rate of LGR5^{+} cells (F), LGR5^{hi} and LGR5^{lo} cells (G), and LGR5$^{hi\text{-}high}$ and LGR5$^{hi\text{-}low}$ cells (H) of irradiated mice (24 h after IR) compared to non-irradiated mice (NIR). Mean values ± SEM are given. Unpaired two-tailed Student's t-test. (I–P) Representative FACS plots of LGR5^{+} cells in freshly isolated basal crypts from irradiated and non-irradiated mice of indicated genotypes. Note the stronger rescue of survival rate of LGR5$^{hi\text{-}high}$ than the LGR5$^{hi\text{-}low}$ cells upon p53 deletion. NIR, non-irradiated; IR, irradiated.

LGR5^{lo} cells (Fig 7A–F and K–M). Reversely, activation of Wnt signaling by treatment with 6-BIO led to a significant increase in radio-sensitivity of both LGR5^{hi} cells and LGR5^{lo} cells compared to control-treated cultures (Me-BIO) (Fig 7G–J and N–P).

Modification of canonical Wnt/β-catenin signaling activity changes the radio-sensitivity of ISPCs *in vivo*

To test whether the modulation of Wnt signal activity would also change the radio-sensitivity of ISPCs *in vivo*, anti-LRP6 antibody was injected to mice shortly before irradiation to transiently inhibit Wnt signaling (Ettenberg *et al*, 2010). Anti-LRP6 antibody injection led to a significant reduction in GFP expression in crypt base stem and progenitor cells (Fig 8A–G) and in *Axin2* expression in freshly isolated Lgr5^{hi} cells compared to vehicle control-injected mice (Supplementary Fig S7F). Notably, single dose of anti-LRP6-antibody injection did not lead to a significant loss of bottom ISPCs though lowering the GFP expression level in these cells (Fig 8H, I and L). Inhibition of Wnt signaling rescued the maintenance in the total number of crypt bottom PCNA^{+} ISPCs in the intestinal epithelium of irradiated mice but most pronounced in the survival of cells in position 1 and 2 of the basal crypt (Fig 8J–L). FACS analysis showed that anti-LRP6 antibody treatment led to a reduction of LGR5^{hi} cells and an increase of LGR5^{lo} cells in non-irradiated mice resulting in an improved maintenance of LGR5^{+} cells after irradiation (Fig 8M–R).

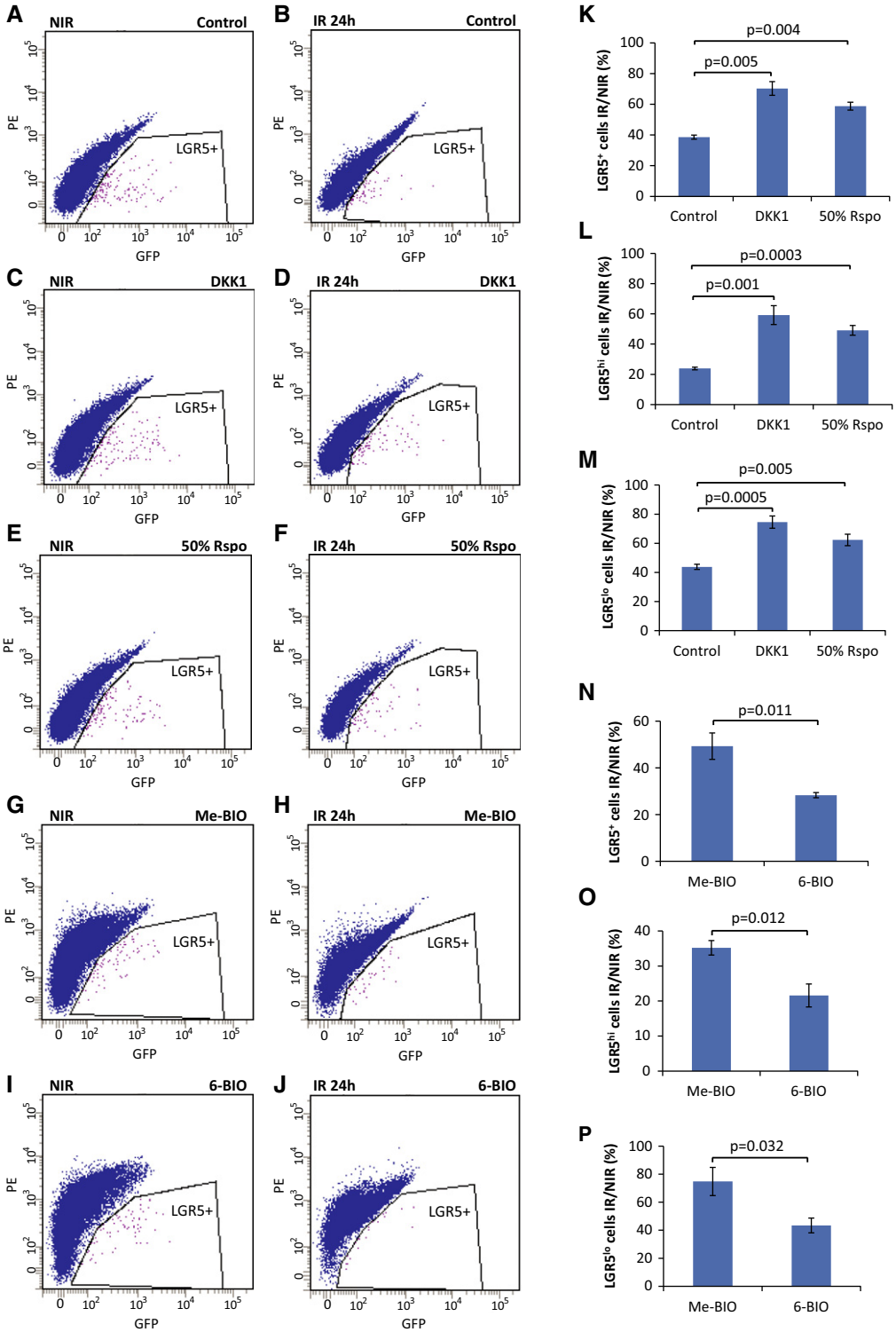

Figure 7. Chemical modification of canonical Wnt/β-catenin signaling activity changes the radio-sensitivity of cultured ISPCs.

Crypts of 2- to 3-month-old LGR5^{ki} mice were cultured and γ-irradiated with 6 Gy on day 10 of culture. Sixteen hours before irradiation, cells were exposed to the indicated treatment (n = 4 independent experiments per group).

A–J Representative FACS plots of indicated treatments are given. NIR, non-irradiated; IR, irradiated.

K–P Flow cytometry analysis of the percentage of LGR5^{+}, LGR5^{hi}, and LGR5^{lo} cells of irradiated cultures (24 h after IR) compared to the percentage in non-irradiated controls (NIR) set to 100%. (K–M) Note that inhibition of Wnt signaling by DKK1 treatment or R-spondin reduction (50% Rspo) partially rescued the decrease in LGR5^{+} cells in irradiated cultures. (N–P) Note that activation of Wnt signaling by 6-BIO treatment aggravated the decrease in LGR5^{+} cells in irradiated cultures. Mean values ± SEM are given. Unpaired two-tailed Student's t-test.

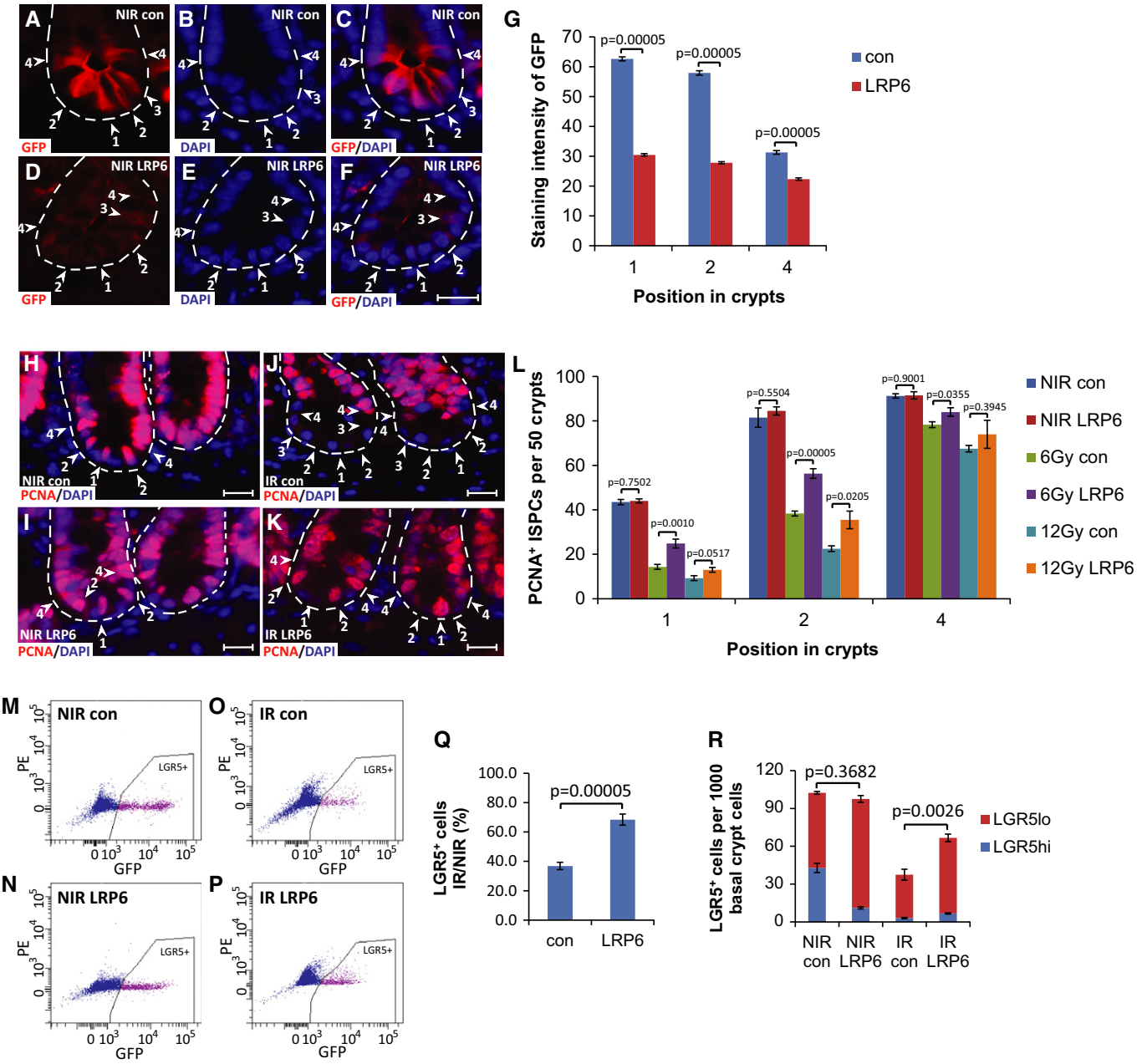

Figure 8. Transient inhibition of canonical Wnt/β-catenin signaling activity decreases radio-sensitivity of ISPCs *in vivo*.

A–G Two-month-old LGR5-GFP^{ki}, *mTerc*$^{+/+}$ mice were i.v. injected with LRP6 neutralization antibody, and IgG serves as a negative control. Thirty-six hours after injection, small intestinal tissue was collected for GFP immunofluorescence staining. (A–F) Representative pictures are given. Dashed lines outline the crypts. Arrowheads and numbers indicate cell positions in the crypts. Scale bar: 20 μm. (G) Quantification of GFP staining intensity of cells at indicated positions in basal crypts (n = 3 mice per group, fifty positively stained cells were measured per mouse). Note the GFP staining intensity was substantially reduced in anti-LRP6 antibody-injected group with intact maintenance of ISPCs at the crypt bottom as shown by DAPI staining.

H–L Two-month-old *mTerc*$^{+/+}$ mice were i.v. injected with anti-LRP6 antibody 12 h before γ-irradiation. Small intestinal tissue was collected at 24 h after IR (n = 3–4 mice per group). IgG serves as a negative control. (H–K) Representative pictures of PCNA staining of small intestine of non-irradiated mice (H, I) or 6 Gy-irradiated mice (J, K). Note the anti-LRP6 antibody injection did not induce loss of CBC cells at position 1 and 2 in non-irradiated mice. Arrowheads and numbers indicate ISPC positions in the crypts. Scale bar: 20 μm. (L) Quantification of PCNA^{+} ISPCs at the indicated positions in basal crypts 24 h after IR with indicated doses or non-irradiated mice.

M–R Two-month-old LGR5-GFP^{ki}, *mTerc*$^{+/+}$ mice were i.v. injected with LRP6 neutralization antibody 12 h before 12 Gy γ-irradiation. IgG serves as a negative control. Small intestinal tissue was collected at 24 h after IR (n = 4 mice per group). (M–P) Representative FACS plots of indicated treatments. (Q) Flow cytometry analysis of the number of LGR5^{+} ISPCs of irradiated mice compared to the number in non-irradiated mice (NIR) set to 100%. (R) Quantification of the number of LGR5^{+}, LGR5^{hi}, and LGR5^{lo} cells of mice with indicated treatment by flow cytometry. Note that the total LGR5^{+} cell frequency was not significantly different between anti-LRP6 antibody-injected and control IgG-injected mice, though the LGR5^{hi} fraction was reduced in the LRP6 antibody-injected group.

Data information: Mean values ± SEM are given. Unpaired two-tailed Student's t-test. NIR, non-irradiated; IR, irradiated; con, control IgG antibody injected; LRP6, anti-LRP6 antibody injected.

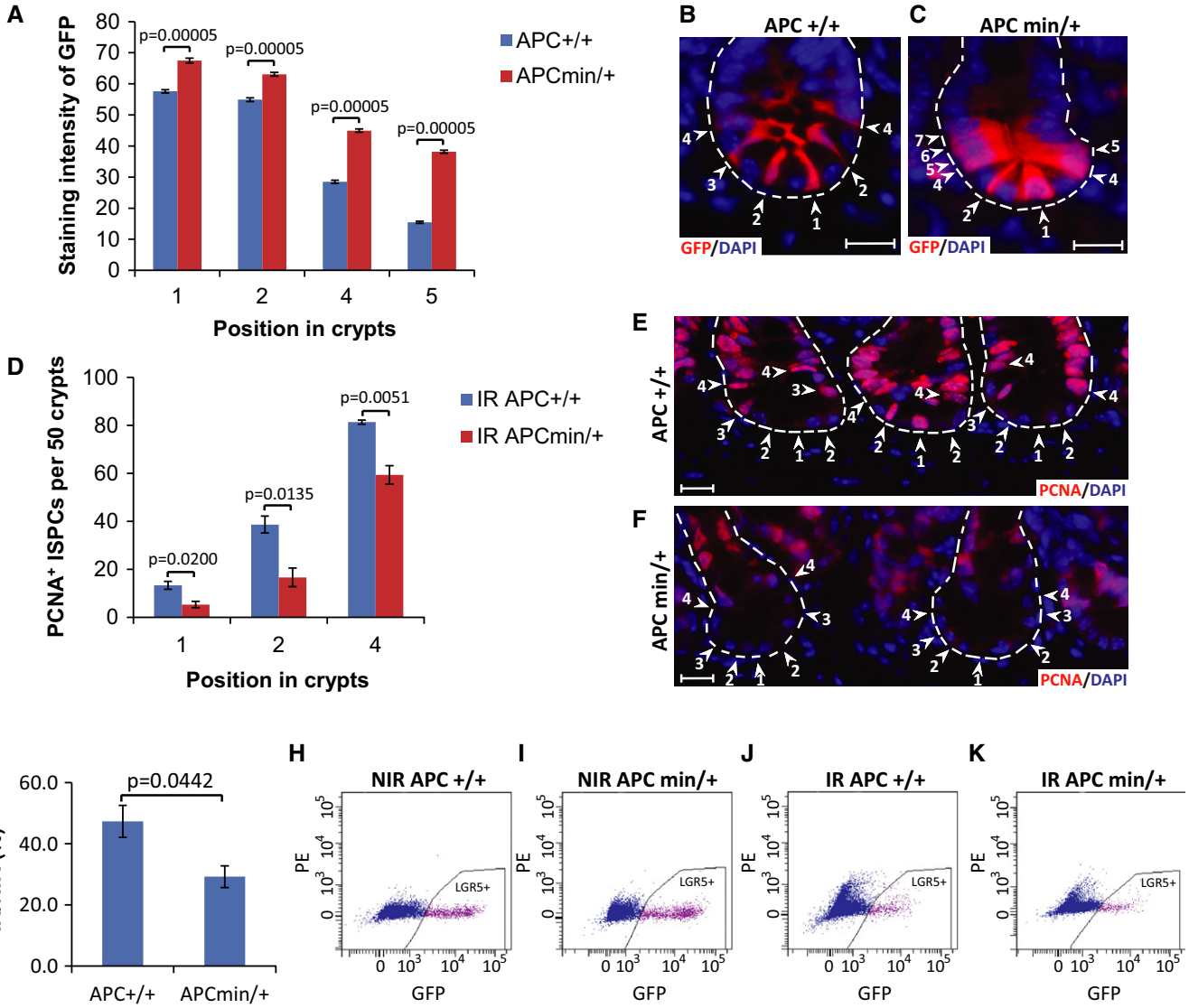

Figure 9. Genetically activating canonical Wnt/β-catenin signaling activity by APC mutation increases the radio-sensitivity of ISPCs *in vivo*.

A–C GFP immunofluorescence staining of small intestine from 2-month-old LGR5-GFP^{ki}, APC$^{+/+}$ mice and LGR5-GFP^{ki}, APC$^{min/+}$ mice. (A) Quantification of GFP staining intensity of cells at indicated positions in basal crypts (n = 3 mice per group, 50 positively stained cells were measured per mouse). Note the GFP staining intensity was increased in APC$^{min/+}$ mice, particularly in position 4 and 5 cells. (B, C) Representative pictures are given. Dashed lines outline the crypts. Arrowheads and numbers indicate cell positions in the crypts. Scale bar: 20 μm.

D–F Two-month-old APC$^{+/+}$ mice and APC$^{min/+}$ mice were exposed to 6 Gy γ-irradiation. Small intestinal tissue was collected at 24 h after IR (n = 3 mice per group). (D) Quantification of PCNA^{+} ISPCs at the indicated positions in basal crypts 24 h after IR. IR, irradiated. (E, F) Representative pictures of PCNA staining are given. Arrowheads and numbers indicate cell positions in the crypts. Scale bar: 20 μm.

G–K Two-month-old LGR5-GFP^{ki}, APC$^{+/+}$ mice and LGR5-GFP^{ki}, APC$^{min/+}$ mice were exposed to 6 Gy γ-irradiation. Small intestinal tissue was collected at 24 h after IR (n = 4 mice per group). (G) Flow cytometry analysis of the number of LGR5^{+} ISPCs of irradiated mice compared to the number in non-irradiated mice (NIR) set to 100%. (H–K) Representative FACS plots of indicated groups are given.

Data information: Mean values ± SEM are given. Unpaired two-tailed Student's t-test. NIR, non-irradiated; IR, irradiated.

To analyze consequences of Wnt activation on IR-induced depletion of ISPCs, APC$^{min/+}$ mice with enhanced Wnt activity (Zeilstra *et al*, 2008) were crossed to LGR5-GFP reporter mice. APC$^{min/+}$ mice exhibited an enhanced GFP expression intensity in position 1–4 cells and even some GFP expression in TA cells above position 4 (Fig 9A–C). Notably, activation of Wnt signaling by genetic mutation of APC led to a greater loss of position 1–4 ISPCs upon irradiation (Fig 9D–F). FACS analysis also showed that IR led to a significantly enhanced depletion of LGR5^{+} cells in the intestinal epithelium of APC$^{min/+}$ mice compared to APC$^{+/+}$ mice (Fig 9G–K).

Discussion

The current study provides the first experimental evidence that cell intrinsic levels of canonical Wnt signaling determine heterogeneity

in the sensitivity of ISPCs to DNA damage. These findings could be relevant for the evolution of stem and progenitor cell dysfunction and the selective survival of aberrant and mutant stem and progenitor cell clones in conditions associated with DNA damage accumulation such as aging and carcinogenesis.

Wnt signaling and stem and progenitor cell aging

This study shows that DNA damage results in the depletion of stem and progenitor cells with intrinsically high levels of Wnt signaling in the intestinal epithelium. There is increasing evidence that Wnt signaling, in addition to being an important factor for self-renewal of stem cells and tissue regeneration, can also contribute to tissue aging. Along these lines, it was shown that over-activation of Wnt in transgenic mice leads to defects in HSC functionality (Kirstetter *et al*, 2006; Scheller *et al*, 2006) and exerts deleterious effects on the maintenance of epithelial stem cells (Castilho *et al*, 2009). Systemic increases in Wnt signaling led to premature aging in Klotho-deficient mice (Liu *et al*, 2007), and parabiosis studies revealed evidence that aging-associated increases in Wnt stimulatory activity in blood serum contribute to the decrease in stem cell functionality and impaired regeneration during aging of wild-type mice (Brack *et al*, 2007).

Despite these evidences that increases in Wnt signaling have adverse effects on stem cell maintenance and tissue aging, the mechanism is still poorly understood. The current study indicates that DNA damage represents a major confounding factor limiting stem cell maintenance in the context of elevated Wnt signaling. The study shows that cell intrinsic heterogeneity in the level of Wnt activity in stem and progenitor cells modulates their sensitivity to DNA damage. High levels of Wnt signaling amplify p53-dependent DNA damage responses and increase stem and progenitor cell apoptosis in response to DNA damage. These findings stand in agreement with previous studies showing that Wnt activity can amplify DNA damage responses in other cell types (Damalas *et al*, 1999; Xu *et al*, 2008; Zhang *et al*, 2011). The current study shows that DNA damage leads to an amplification of Wnt signaling in ISPCs at early time points after DNA damage suggesting a feed-forward loop of DNA damage inducing Wnt signaling, which in turn amplifies the DNA damage response (DDR). This signal-enhancing forward loop contributes to the induction of DNA damage checkpoints in ISPCs. In line with this interpretation, this study shows that elevating Wnt signaling increases radio-sensitivity of ISPCs, while inhibition of Wnt signaling reduces the radio-sensitivity of ISPCs both *in vitro* and *in vivo*.

This study supports a model indicating that stem and progenitor cells with intrinsically low Wnt signaling activity represent a backup population ensuring recovery of tissue maintenance and survival in response to acute or chronic DNA damage. It was demonstrated by live cell imaging studies that +4 cells consist of a mixture of early TA cells (LGR5-GFP-negative) and LGR5-GFP$^+$ stem cells (Ritsma *et al*, 2014). In addition, lineage-tracing experiments revealed that Dll1$^+$ TA cells revert to stem cells in response to severe tissue damage (van Es *et al*, 2012). However, LGR5$^+$ cells were shown to be essential for survival of mice in response to IR, and reversion of Dll1$^+$ TA cells into stem cells is not sufficient for mouse survival in response to IR (van Es *et al*, 2012; Metcalfe *et al*, 2014). The current study shows that within the fraction of LGR5$^+$ cells, the cells with low LGR5 expression and low Wnt signaling activity (low *Msi1*, low *Axin2*) preferentially survive in response to DNA damage. This holds true for FACS-gated subpopulation of LGR5-high positive cells (LGR5$^{hi\text{-}high}$ cells being more sensitive to IR than LGR5$^{hi\text{-}low}$ cells) and coincides with preferential survival of GFP-positive cells in position 4 of the basal crypt. Together, these results stand in accordance with the concept that niche-dependent local signals and cell intrinsic Wnt signaling modulate the survival of ISPCs in response to DNA damage. Based on our study, it is conceivable that Wnt signaling has a dual role in maintenance of the intestinal epithelium in response to acute DNA damage. While the lowering of Wnt signaling can enhance the survival of ISPCs in response to DNA damage, the elevation of Wnt signals appears to be beneficial for the regenerative phase following the acute damage (Zhou *et al*, 2013). This latter process likely includes pro-regenerative effects at the progenitor cell level. Along these lines, it was shown that Wnt activation promotes radio-resistance of progenitor cells in primary mammary epithelial cell cultures (Woodward *et al*, 2007).

Wnt signaling and maintenance of stem cells and cancer stem cells

An activation of Wnt signaling represents one of the hallmark features of cancer (Polakis, 2000; Holland *et al*, 2013) including the development of malignancies in the hematopoietic system and the intestinal epithelium (Reya & Clevers, 2005). Studies on the role of Wnt signaling in the maintenance of adult, non-transformed stem cells revealed that Wnt activity is required for stem cell maintenance, but over-activation of Wnt leads to stem cell depletion (Reya *et al*, 2003; Fevr *et al*, 2007; Fleming *et al*, 2008; Luis *et al*, 2009; de Lau *et al*, 2011). These previous data point to the existence of checkpoints that limit self-renewal of stem cells with abnormally increased Wnt activity. The current study shows that higher levels of Wnt signaling increase the sensitivity of stem and progenitor cells to DNA damage in the intestinal epithelium. Since DNA damage accumulates in response to proliferation of cancer stem cells (Viale *et al*, 2009), it is conceivable that Wnt-induced amplification of DNA damage signals in cancer stem cells may act as a tumor suppressor mechanism. The over-activation of Wnt signaling in cancers indicates that tumor stem cells escape Wnt-dependent amplification of DNA damage signals possibly involving the depletion of DNA damage checkpoint genes, such as p53. Along these lines, it has been observed that p53 inactivation promotes the progression of tumors induced by enhanced Wnt signaling in mouse models and human cancer cells (Donehower *et al*, 1995; Halberg *et al*, 2000; Kim *et al*, 2011). Interestingly, interspecies comparison on mouse and human intestinal carcinogenesis supports a model indicating that an optimal level of moderately increased Wnt signaling promotes the formation of tumorigenic lesion while excessive high levels of Wnt activity do not (Leedham *et al*, 2013). It is tempting to speculate that Wnt-dependent sensitizing of intestinal tumor stem cells to DNA damage could contribute to the selection of only moderately increased Wnt activity during tumor formation.

Current experiments support the notion that heterogeneity in Wnt signaling activity in non-transformed ISPCs originates from the position of the stem cells in the stem cell niche. CBCs that are located in between the Paneth cells at the crypt base exhibit higher

Wnt signaling than those cells located above the upper most Paneth cells flanked by only one or two Paneth cells. The increased DNA damage resistance of ISPCs in stem cell niches with reduced Wnt stimulatory activity could enable the survival of initiated tumor cells, which often exhibit an increase in DNA damage and an activation of DNA damage checkpoints (Ye *et al*, 2007). In addition, there is evidence that the tumor stroma influences heterogeneity in Wnt signaling activity in cancer cells (Vermeulen *et al*, 2010). It is tempting to speculate that the heterogeneity of Wnt activity in tumor cells would also influence the sensitivity of established tumors to DNA-damaging agents.

Together, the current study provides the first experimental evidence that the level of Wnt signaling activity represents a major confounding factor modulating the sensitivity of ISPCs to DNA damage. Selective survival of stem and progenitor cells with low Wnt signaling activity could influence the selection of aberrant stem and progenitor cells in the context of DNA damage during aging and carcinogenesis. This study also shows that treatment-induced modification of canonical Wnt signaling activity changes the radiosensitivity of ISPCs. These data support the concept that modulation of canonical Wnt signaling could represent a novel therapeutic target to influence the survival of non-transformed stem cells and possibly also of tumor stem cells in response to DNA-damaging agents.

Materials and Methods

Mice

Mice were bred and maintained in the animal facilities of Ulm University and Leibniz Institute for Age Research on a standard diet and on a 12-h light–dark cycle. Mice were monitored by weekly inspection. All mice were maintained on a C57BL/6J background. $mTerc^{-/-}$ mice were intercrossed to generate G3 $mTerc^{-/-}$ mice. *Lgr5-EGFP-IRES-CreERT2* mice were kindly provided by Hans Clevers. *Lgr5-EGFP-IRES-CreERT2* mice were crossed with $mTerc^{-/-}$ mice and intercrossed to generate $LGR5^{ki}$; G3 $mTerc^{-/-}$ mice. P53 knockout mice and $APC^{min/+}$ mice were bought from Jackson Laboratory, and they were crossed with *Lgr5-EGFP-IRES-CreERT2* mice, respectively. C57BL/6J wild-type mice were from Janvier Labs, France. All mice experiments were approved by the state government of Baden-Württemberg (Protocol Number 35/9185.81-3/919) and Thüringen (Protocol Number 03-006/13).

RNA isolation and cDNA synthesis

Total RNA was isolated from freshly sorted cells or crypts by using MagMAX™-96 Viral RNA Isolation kit (Ambion). DNA digestion step was included during the RNA purification process. Reverse transcriptions were performed to synthesize first-strand DNA by using the GoScript reverse transcription system (Promega).

Quantitative real-time PCR

qPCR was performed with an ABI 7300 Real-Time PCR System (Applied Biosystems) in duplicates or triplicates from at least three biological samples. Primer sets for the detection of single genes are listed in Supplementary Table S1. iTaq SYBR Green supermix with Rox (Bio-Rad) was used. Expression of genes was normalized to *GAPDH* in each sample.

Flow cytometry

For $LGR5\text{-}GFP^{ki}$ mice crypt cell flow cytometry, crypt single-cell suspension was prepared as described (Sato *et al*, 2009). For cell cycle analysis, Cytofix/Cytoperm Kit (BD Biosciences) was used. Data acquisition and cell sorting were performed on FACS LSRII and FACS AriaIII (BD Biosciences). Data were analyzed with the BD FACS Diva software (BD Biosciences).

Immunofluorescence staining

5-μm paraffin sections of small intestine were used for immunofluorescence staining. Antibodies used were the following: PCNA (Calbiochem), Ki-67 (Monosan), GFP (SantaCruz), Msi1 (eBioscience), anti-mouse-IgG-Cy3 secondary antibody (Invitrogen), anti-mouse-IgG-FITC secondary antibody (Invitrogen), anti-rat-IgG-FITC (Invitrogen), and anti-rabbit-IgG-Cy3 secondary antibody (Invitrogen).

Restrict counting regime of ISPCs was performed as following: Positions were counted starting from the lowest position of the basal crypt, which was defined as position 1. The neighboring position above the last Paneth cell was defined as position 4. ISPCs of both sides of the crypt were counted. Staining intensity of GFP and Msi1 was measured by ImageJ software in the Cy3 channel and FITC channel, respectively.

In situ hybridization

Eight-micrometer paraffin sections of small intestine were used for *in situ* hybridization. The staining was done as described (Sperka *et al*, 2011).

TUNEL assay

TUNEL assay was performed using the *In Situ* Cell Death Detection Kit, Fluorescein (Roche) according to the manufacturer's instructions.

Western blot

Equal numbers of cells were FACS-sorted and lysed with Laemmli sample buffer (50 mM Trisbase pH 6.8, 4% SDS, 0.04% bromophenolblue, 20% glycerol). Whole-cell lysates were boiled and loaded on 10 or 12% SDS–PAGE gel for electrophoresis. Following antibodies were used for immunoblotting: phospho-p53 (Ser15) (1:1,000; Cell Signaling), cleaved caspase-3 (1:1,000; Cell Signaling), and beta-actin (1:10,000; Sigma).

Cell culture

Crypt culture was performed as previously described (Sperka *et al*, 2011). Briefly, isolated crypts were resuspended in cold Matrigel (BD) containing Y27632 (Abcam), R-spondin, mEGF (PeproTech), Noggin (PeproTech), and penicillin/streptomycin and plated in 24-well plate at density of 200 crypts, 50 μl per well. The plate was incubated at 37°C for 5 min, and then, 500 μl of advanced DMEM/F

12 medium (Invitrogen) containing B27 (Invitrogen), N2 supplement (Invitrogen), and 1.25 mM N-acetylcystein was added to each well to cover the Matrigel. In the culture system, final concentrations of the following components were R-spondin 1 μg/ml, mEGF 50 ng/ml, and Noggin 100 ng/ml. Y27632 10 μM was included in the first 3 days after seeding. The medium containing growth factors was changed every 3 days, and crypts were passaged every 9 days. Modification of Wnt activity was performed on day 9, 16 h before irradiation. DKK1 protein (R&D Systems) was used at a final concentration of 500 ng/ml. Rspo was prepared as previously described (Sperka *et al*, 2011). Six-BIO (Calbiochem) or Me-BIO (Calbiochem) was dissolved in DMSO and used at a final concentration of 20 nM. Single cell culture was performed as previously described (Sato *et al*, 2011). Briefly, sorted single $LGR5^{hi}$ or $LGR5^{lo}$ cells were pelleted and embedded in Matrigel, followed by seeding on a 96-well plate (round bottom). Culture medium as described above with addition of 100 ng/ml Wnt3a (R&D Systems) was overlaid. Growth factors were added every other day, and culture medium was changed every 4 days.

Microarray analysis

RNA quality was controlled by the 2100 Bioanalyzer (Agilent Technologies). Quality-proved RNA with a RIN value higher than 9.0 was used for gene expression analysis, which was performed using the SurePrint G3 Mouse GE 8x60K (Design ID 028005) Microarray Kit (Agilent Technologies). 50 ng of each sample was labeled with the Low Input Quick Amp Labeling Kit (Agilent Technologies) according to the manufacturer's instructions. Slides were scanned using a microarray scanner (Agilent Technologies). All expression data were deposited in Gene Expression Omnibus (GEO accession number GSE49461).

Anti-LRP6 antibody

The LRP6 neutralization antibody was kindly provided by Dr. Seth A. Ettenberga and Michael P. Daley and applied to mice according to previous publications (Ettenberg *et al*, 2010). Briefly, anti-LRP6 antibody (BpAb A7/B2) was injected intravenously with a single dose of 5 mg/kg 12 h before irradiation. Equal amount of IgG antibody was injected to control mice.

Statistics

SPSS 11.5 and GraphPad Prism 6 softwares were used for statistical analysis. The unpaired two-tailed Student's *t*-test was used to calculate *P*-values for all datasets except for the microarray analysis where Wilcoxon test was used.

Supplementary information for this article is available online: http://emboj.embopress.org

Acknowledgements

This work was supported by the German Federal Ministry of Education and Research BMBF within its joint research project SyStaR (KLR, MK, HAK), by the EU (ERC to KLR: 323136—Stem Cell Geronto Genes) and by the International Graduate School in Molecular Medicine Ulm, funded by the Excellence Initiative of the German Federal and State Governments (GSC270).

Author contributions

ST and DT performed and analyzed majority of all experiments, including crypt isolation and culture, $LGR5^{hi}$ and $LGR5^{lo}$ cell purification, RNA isolation and qPCR, flow cytometry, intestinal tissue staining and counting, irradiation, and Western blot. YM did anti-LRP6 antibody injection and helped in FACS experiments. TS and OO gave suggestions and helped in some crypt isolation experiments. AL performed microarray experiment. VS provided technical assistance for mouse experiments. JK and HAK performed microarray analysis. MK and KLR conceived and designed the experiments. The manuscript was written by ST, MK, and KLR and commented on by all other authors.

Conflict of interest

The authors declare that they have no conflict of interest.

References

van Amerongen R, Bowman AN, Nusse R (2012) Developmental stage and time dictate the fate of Wnt/beta-catenin-responsive stem cells in the mammary gland. *Cell Stem Cell* 11: 387 – 400

Armanios MY, Chen JJ, Cogan JD, Alder JK, Ingersoll RG, Markin C, Lawson WE, Xie M, Vulto I, Phillips JA III, Lansdorp PM, Greider CW, Loyd JE (2007) Telomerase mutations in families with idiopathic pulmonary fibrosis. *N Engl J Med* 356: 1317 – 1326

Barker N, van Es JH, Kuipers J, Kujala P, van den Born M, Cozijnsen M, Haegebarth A, Korving J, Begthel H, Peters PJ, Clevers H (2007) Identification of stem cells in small intestine and colon by marker gene Lgr5. *Nature* 449: 1003 – 1007

Barker N, Ridgway RA, van Es JH, van de Wetering M, Begthel H, van den Born M, Danenberg E, Clarke AR, Sansom OJ, Clevers H (2009) Crypt stem cells as the cells-of-origin of intestinal cancer. *Nature* 457: 608 – 611

Barker N, van Oudenaarden A, Clevers H (2012) Identifying the stem cell of the intestinal crypt: strategies and pitfalls. *Cell Stem Cell* 11: 452 – 460

Begus-Nahrmann Y, Lechel A, Obenauf AC, Nalapareddy K, Peit E, Hoffmann E, Schlaudraff F, Liss B, Schirmacher P, Kestler H, Danenberg E, Barker N, Clevers H, Speicher MR, Rudolph KL (2009) p53 deletion impairs clearance of chromosomal-instable stem cells in aging telomere-dysfunctional mice. *Nat Genet* 41: 1138 – 1143

Brack AS, Conboy MJ, Roy S, Lee M, Kuo CJ, Keller C, Rando TA (2007) Increased Wnt signaling during aging alters muscle stem cell fate and increases fibrosis. *Science* 317: 807 – 810

Busque L, Patel JP, Figueroa ME, Vasanthakumar A, Provost S, Hamilou Z, Mollica L, Li J, Viale A, Heguy A, Hassimi M, Socci N, Bhatt PK, Gonen M, Mason CE, Melnick A, Godley LA, Brennan CW, Abdel-Wahab O, Levine RL (2012) Recurrent somatic TET2 mutations in normal elderly individuals with clonal hematopoiesis. *Nat Genet* 44: 1179 – 1181

Castilho RM, Squarize CH, Chodosh LA, Williams BO, Gutkind JS (2009) mTOR mediates Wnt-induced epidermal stem cell exhaustion and aging. *Cell Stem Cell* 5: 279 – 289

Choudhury AR, Ju Z, Djojosubroto MW, Schienke A, Lechel A, Schaetzlein S, Jiang H, Stepczynska A, Wang C, Buer J, Lee HW, von Zglinicki T, Ganser A, Schirmacher P, Nakauchi H, Rudolph KL (2007) Cdkn1a deletion improves stem cell function and lifespan of mice with dysfunctional telomeres without accelerating cancer formation. *Nat Genet* 39: 99 – 105

Damalas A, Ben-Ze'ev A, Simcha I, Shtutman M, Leal JF, Zhurinsky J, Geiger B, Oren M (1999) Excess beta-catenin promotes accumulation of transcriptionally active p53. *EMBO J* 18: 3054 – 3063

Donehower LA, Godley LA, Aldaz CM, Pyle R, Shi YP, Pinkel D, Gray J, Bradley A, Medina D, Varmus HE (1995) Deficiency of p53 accelerates mammary tumorigenesis in Wnt-1 transgenic mice and promotes chromosomal instability. *Genes Dev* 9: 882 – 895

van Es JH, Sato T, van de Wetering M, Lyubimova A, Nee AN, Gregorieff A, Sasaki N, Zeinstra L, van den Born M, Korving J, Martens AC, Barker N, van Oudenaarden A, Clevers H (2012) Dll1$^+$ secretory progenitor cells revert to stem cells upon crypt damage. *Nat Cell Biol* 14: 1099 – 1104

Ettenberg SA, Charlat O, Daley MP, Liu S, Vincent KJ, Stuart DD, Schuller AG, Yuan J, Ospina B, Green J, Yu Q, Walsh R, Li S, Schmitz R, Heine H, Bilic S, Ostrom L, Mosher R, Hartlepp KF, Zhu Z *et al* (2010) Inhibition of tumorigenesis driven by different Wnt proteins requires blockade of distinct ligand-binding regions by LRP6 antibodies. *Proc Natl Acad Sci USA* 107: 15473 – 15478

Fevr T, Robine S, Louvard D, Huelsken J (2007) Wnt/beta-catenin is essential for intestinal homeostasis and maintenance of intestinal stem cells. *Mol Cell Biol* 27: 7551 – 7559

Fleming HE, Janzen V, Lo Celso C, Guo J, Leahy KM, Kronenberg HM, Scadden DT (2008) Wnt signaling in the niche enforces hematopoietic stem cell quiescence and is necessary to preserve self-renewal in vivo. *Cell Stem Cell* 2: 274 – 283

van der Flier LG, van Gijn ME, Hatzis P, Kujala P, Haegebarth A, Stange DE, Begthel H, van den Born M, Guryev V, Oving I, van Es JH, Barker N, Peters PJ, van de Wetering M, Clevers H (2009) Transcription factor achaete scute-like 2 controls intestinal stem cell fate. *Cell* 136: 903 – 912

Genovese G, Kähler AK, Handsaker RE, Lindberg J, Rose SA, Bakhoum SF, Chambert K, Mick E, Neale BM, Fromer M, Purcell SM, Svantesson O, Landén M, Höglund M, Lehmann S, Gabriel SB, Moran JL, Lander ES, Sullivan PF, Sklar P *et al* (2014) Clonal hematopoiesis and blood-cancer risk inferred from blood DNA sequence. *N Engl J Med* 371: 2477 – 2487

Halberg RB, Katzung DS, Hoff PD, Moser AR, Cole CE, Lubet RA, Donehower LA, Jacoby RF, Dove WF (2000) Tumorigenesis in the multiple intestinal neoplasia mouse: redundancy of negative regulators and specificity of modifiers. *Proc Natl Acad Sci USA* 97: 3461 – 3466

Herbig U, Ferreira M, Condel L, Carey D, Sedivy JM (2006) Cellular senescence in aging primates. *Science* 311: 1257

Hoeijmakers JH (2009) DNA damage, aging, and cancer. *N Engl J Med* 361: 1475 – 1485

Holland JD, Klaus A, Garratt AN, Birchmeier W (2013) Wnt signaling in stem and cancer stem cells. *Curr Opin Cell Biol* 25: 254 – 264

Huang J, Zhang Y, Bersenev A, O'Brien WT, Tong W, Emerson SG, Klein PS (2009) Pivotal role for glycogen synthase kinase-3 in hematopoietic stem cell homeostasis in mice. *J Clin Invest* 119: 3519 – 3529

Itzkovitz S, Lyubimova A, Blat IC, Maynard M, van Es J, Lees J, Jacks T, Clevers H, van Oudenaarden A (2012) Single-molecule transcript counting of stem-cell markers in the mouse intestine. *Nat Cell Biol* 14: 106 – 114

Jaiswal S, Fontanillas P, Flannick J, Manning A, Grauman PV, Mar BG, Lindsley RC, Mermel CH, Burtt N, Chavez A, Higgins JM, Moltchanov V, Kuo FC, Kluk MJ, Henderson B, Kinnunen L, Koistinen HA, Ladenvall C, Getz G, Correa A *et al* (2014) Age-related clonal hematopoiesis associated with adverse outcomes. *N Engl J Med* 371: 2488 – 2498

Jan M, Snyder TM, Corces-Zimmerman MR, Vyas P, Weissman IL, Quake SR, Majeti R (2012) Clonal evolution of preleukemic hematopoietic stem cells precedes human acute myeloid leukemia. *Sci Transl Med* 4: 149ra118

Jiang H, Schiffer E, Song Z, Wang J, Zurbig P, Thedieck K, Moes S, Bantel H, Saal N, Jantos J, Brecht M, Jeno P, Hall MN, Hager K, Manns MP, Hecker H, Ganser A, Dohner K, Bartke A, Meissner C *et al* (2008) Proteins induced by telomere dysfunction and DNA damage represent biomarkers of human aging and disease. *Proc Natl Acad Sci USA* 105: 11299 – 11304

Kayahara T, Sawada M, Takaishi S, Fukui H, Seno H, Fukuzawa H, Suzuki K, Hiai H, Kageyama R, Okano H, Chiba T (2003) Candidate markers for stem and early progenitor cells, Musashi-1 and Hes1, are expressed in crypt base columnar cells of mouse small intestine. *FEBS Lett* 535: 131 – 135

Kim NH, Kim HS, Kim NG, Lee I, Choi HS, Li XY, Kang SE, Cha SY, Ryu JK, Na JM, Park C, Kim K, Lee S, Gumbiner BM, Yook JI, Weiss SJ (2011) p53 and microRNA-34 are suppressors of canonical Wnt signaling. *Sci Signal* 4: ra71

Kim TH, Escudero S, Shivdasani RA (2012) Intact function of Lgr5 receptor-expressing intestinal stem cells in the absence of Paneth cells. *Proc Natl Acad Sci USA* 109: 3932 – 3937

Kirstetter P, Anderson K, Porse BT, Jacobsen SE, Nerlov C (2006) Activation of the canonical Wnt pathway leads to loss of hematopoietic stem cell repopulation and multilineage differentiation block. *Nat Immunol* 7: 1048 – 1056

Lane SW, Sykes SM, Al-Shahrour F, Shterental S, Paktinat M, Lo Celso C, Jesneck JL, Ebert BL, Williams DA, Gilliland DG (2010) The Apc(min) mouse has altered hematopoietic stem cell function and provides a model for MPD/MDS. *Blood* 115: 3489 – 3497

de Lau W, Barker N, Low TY, Koo BK, Li VS, Teunissen H, Kujala P, Haegebarth A, Peters PJ, van de Wetering M, Stange DE, van Es JE, Guardavaccaro D, Schasfoort RB, Mohri Y, Nishimori K, Mohammed S, Heck AJ, Clevers H (2011) Lgr5 homologues associate with Wnt receptors and mediate R-spondin signalling. *Nature* 476: 293 – 297

Leedham SJ, Rodenas-Cuadrado P, Howarth K, Lewis A, Mallappa S, Segditsas S, Davis H, Jeffery R, Rodriguez-Justo M, Keshav S, Travis SP, Graham TA, East J, Clark S, Tomlinson IP (2013) A basal gradient of Wnt and stem-cell number influences regional tumour distribution in human and mouse intestinal tracts. *Gut* 62: 83 – 93

Liu H, Fergusson MM, Castilho RM, Liu J, Cao L, Chen J, Malide D, Rovira II, Schimel D, Kuo CJ, Gutkind JS, Hwang PM, Finkel T (2007) Augmented Wnt signaling in a mammalian model of accelerated aging. *Science* 317: 803 – 806

Liu L, Rando TA (2011) Manifestations and mechanisms of stem cell aging. *J Cell Biol* 193: 257 – 266

Luis TC, Weerkamp F, Naber BA, Baert MR, de Haas EF, Nikolic T, Heuvelmans S, De Krijger RR, van Dongen JJ, Staal FJ (2009) Wnt3a deficiency irreversibly impairs hematopoietic stem cell self-renewal and leads to defects in progenitor cell differentiation. *Blood* 113: 546 – 554

Metcalfe C, Kljavin NM, Ybarra R, de Sauvage FJ (2014) Lgr5$^+$ stem cells are indispensable for radiation-induced intestinal regeneration. *Cell Stem Cell* 14: 149 – 159

Munoz J, Stange DE, Schepers AG, van de Wetering M, Koo BK, Itzkovitz S, Volckmann R, Kung KS, Koster J, Radulescu S, Myant K, Versteeg R, Sansom OJ, van Es JH, Barker N, van Oudenaarden A, Mohammed S, Heck AJ, Clevers H (2012) The Lgr5 intestinal stem cell signature: robust expression of proposed quiescent "+4" cell markers. *EMBO J* 31: 3079 – 3091

Polakis P (2000) Wnt signaling and cancer. *Genes Dev* 14: 1837 – 1851

Ren B, Cam H, Takahashi Y, Volkert T, Terragni J, Young RA, Dynlacht BD (2002) E2F integrates cell cycle progression with DNA repair, replication, and G(2)/M checkpoints. *Genes Dev* 16: 245 – 256

Reya T, Duncan AW, Ailles L, Domen J, Scherer DC, Willert K, Hintz L, Nusse R, Weissman IL (2003) A role for Wnt signalling in self-renewal of haematopoietic stem cells. *Nature* 423: 409 – 414

Reya T, Clevers H (2005) Wnt signalling in stem cells and cancer. *Nature* 434: 843 – 850

Rezza A, Skah S, Roche C, Nadjar J, Samarut J, Plateroti M (2010) The overexpression of the putative gut stem cell marker Musashi-1 induces tumorigenesis through Wnt and Notch activation. *J Cell Sci* 123: 3256 – 3265

Ritsma L, Ellenbroek SI, Zomer A, Snippert HJ, de Sauvage FJ, Simons BD, Clevers H, van Rheenen J (2014) Intestinal crypt homeostasis revealed at single-stem-cell level by in vivo live imaging. *Nature* 507: 362 – 365

Rossi DJ, Bryder D, Seita J, Nussenzweig A, Hoeijmakers J, Weissman IL (2007) Deficiencies in DNA damage repair limit the function of haematopoietic stem cells with age. *Nature* 447: 725 – 729

Rube CE, Fricke A, Widmann TA, Furst T, Madry H, Pfreundschuh M, Rube C (2011) Accumulation of DNA damage in hematopoietic stem and progenitor cells during human aging. *PLoS ONE* 6: e17487

Rudolph KL, Chang S, Lee HW, Blasco M, Gottlieb GJ, Greider C, DePinho RA (1999) Longevity, stress response, and cancer in aging telomerase-deficient mice. *Cell* 96: 701 – 712

Sato T, Vries RG, Snippert HJ, van de Wetering M, Barker N, Stange DE, van Es JH, Abo A, Kujala P, Peters PJ, Clevers H (2009) Single Lgr5 stem cells build crypt-villus structures in vitro without a mesenchymal niche. *Nature* 459: 262 – 265

Sato T, van Es JH, Snippert HJ, Stange DE, Vries RG, van den Born M, Barker N, Shroyer NF, van de Wetering M, Clevers H (2011) Paneth cells constitute the niche for Lgr5 stem cells in intestinal crypts. *Nature* 469: 415 – 418

Schaetzlein S, Kodandaramireddy NR, Ju Z, Lechel A, Stepczynska A, Lilli DR, Clark AB, Rudolph C, Kuhnel F, Wei K, Schlegelberger B, Schirmacher P, Kunkel TA, Greenberg RA, Edelmann W, Rudolph KL (2007) Exonuclease-1 deletion impairs DNA damage signaling and prolongs lifespan of telomere-dysfunctional mice. *Cell* 130: 863 – 877

Scheller M, Huelsken J, Rosenbauer F, Taketo MM, Birchmeier W, Tenen DG, Leutz A (2006) Hematopoietic stem cell and multilineage defects generated by constitutive beta-catenin activation. *Nat Immunol* 7: 1037 – 1047

Sperka T, Song Z, Morita Y, Nalapareddy K, Guachalla LM, Lechel A, Begus-Nahrmann Y, Burkhalter MD, Mach M, Schlaudraff F, Liss B, Ju Z, Speicher MR, Rudolph KL (2011) Puma and p21 represent cooperating checkpoints limiting self-renewal and chromosomal instability of somatic stem cells in response to telomere dysfunction. *Nat Cell Biol* 14: 73 – 79

Sperka T, Wang J, Rudolph KL (2012) DNA damage checkpoints in stem cells, ageing and cancer. *Nat Rev Mol Cell Biol* 13: 579 – 590

Tumpel S, Rudolph KL (2012) The role of telomere shortening in somatic stem cells and tissue aging: lessons from telomerase model systems. *Ann N Y Acad Sci* 1266: 28 – 39

Vermeulen L, De Sousa EMF, van der Heijden M, Cameron K, de Jong JH, Borovski T, Tuynman JB, Todaro M, Merz C, Rodermond H, Sprick MR, Kemper K, Richel DJ, Stassi G, Medema JP (2010) Wnt activity defines colon cancer stem cells and is regulated by the microenvironment. *Nat Cell Biol* 12: 468 – 476

Viale A, De Franco F, Orleth A, Cambiaghi V, Giuliani V, Bossi D, Ronchini C, Ronzoni S, Muradore I, Monestiroli S, Gobbi A, Alcalay M, Minucci S, Pelicci PG (2009) Cell-cycle restriction limits DNA damage and maintains self-renewal of leukaemia stem cells. *Nature* 457: 51 – 56

Welch JS, Ley TJ, Link DC, Miller CA, Larson DE, Koboldt DC, Wartman LD, Lamprecht TL, Liu F, Xia J, Kandoth C, Fulton RS, McLellan MD, Dooling DJ, Wallis JW, Chen K, Harris CC, Schmidt HK, Kalicki-Veizer JM, Lu C *et al* (2012) The origin and evolution of mutations in acute myeloid leukemia. *Cell* 150: 264 – 278

Woodward WA, Chen MS, Behbod F, Alfaro MP, Buchholz TA, Rosen JM (2007) WNT/beta-catenin mediates radiation resistance of mouse mammary progenitor cells. *Proc Natl Acad Sci USA* 104: 618 – 623

Xie M, Lu C, Wang J, McLellan MD, Johnson KJ, Wendl MC, McMichael JF, Schmidt HK, Yellapantula V, Miller CA, Ozenberger BA, Welch JS, Link DC, Walter MJ, Mardis ER, Dipersio JF, Chen F, Wilson RK, Ley TJ, Ding L (2014) Age-related mutations associated with clonal hematopoietic expansion and malignancies. *Nat Med* 20: 1472 – 1478

Xu M, Yu Q, Subrahmanyam R, Difilippantonio MJ, Ried T, Sen JM (2008) Beta-catenin expression results in p53-independent DNA damage and oncogene-induced senescence in prelymphomagenic thymocytes in vivo. *Mol Cell Biol* 28: 1713 – 1723

Ye X, Zerlanko B, Kennedy A, Banumathy G, Zhang R, Adams PD (2007) Downregulation of Wnt signaling is a trigger for formation of facultative heterochromatin and onset of cell senescence in primary human cells. *Mol Cell* 27: 183 – 196

Zeilstra J, Joosten SP, Dokter M, Verwiel E, Spaargaren M, Pals ST (2008) Deletion of the WNT target and cancer stem cell marker CD44 in Apc(Min/$^{+}$) mice attenuates intestinal tumorigenesis. *Cancer Res* 68: 3655 – 3661

Zhang DY, Wang HJ, Tan YZ (2011) Wnt/beta-catenin signaling induces the aging of mesenchymal stem cells through the DNA damage response and the p53/p21 pathway. *PLoS ONE* 6: e21397

Zhou WJ, Geng ZH, Spence JR, Geng JG (2013) Induction of intestinal stem cells by R-spondin 1 and Slit2 augments chemoradioprotection. *Nature* 501: 107 – 111

